New tools for *Euglena*: detection of paramylon and chlorophyll by flow cytometry

Patrick Alexander da Roza

Supervisor: Professor Helena Nevalainen

Associate supervisors: Dr Angela Sun and Associate Professor Anwar Sunna

Department of Molecular Sciences,
Macquarie University

A thesis submitted in fulfilment of the degree of

Master of Research

9 October 2017

Table of Contents

Abstract

Euglena gracilis is a single celled flagellate protist that has garnered industrial interest due its production of paramylon, a crystalline β-1,3-glucan which has been found to have numerous medical properties and potential as a beneficial source of dietary fibre. Traditional biochemical methods of quantifying paramylon have been used extensively but are time consuming and low-throughput. Fluorescence-based methods provide a powerful alternative platform for detection of compounds and screening of desirable strains. The aim of the current research was to develop a method to fluorescently label intracellular paramylon granules in *E. gracilis* and explore the use of flow cytometry (FCM) to monitor paramylon content and chlorophyll content in *E. gracilis* cells during cultivation. Paramylon granules were labelled with the aniline blue dye and assessed via fluorescence and confocal microscopy, and FCM was implemented for high-throughput detection. Novel fluorescent labelling of intracellular paramylon granules was achieved and FCM was successfully utilised for the monitoring of paramylon, chlorophyll and metabolic state of *E. gracilis* during cultivation. Flow cytometry shows promise for algal research and is presented here as a novel tool for detection of paramylon content and monitoring of metabolic state in *E. gracilis,* opening new possibilities for the development of *Euglena* biotechnology.

Declaration

The work presented in this thesis was carried out in the fulfilment of the degree of Master of Research at Macquarie University. This material has not been submitted for assessment or in the attainment of qualifications to any other university or institution.

This thesis is my own original work, undertaken by me between January 2017 and October 2017. It contains no material previously written or published. Contributions made by other authors have been cited with references to the literature. Assistance and instructions made by others have been acknowledged.

Research was undertaken with approval as a Notifiable Low Risk Dealing by the Institutional Biosafety Committee (IBC), effective 13th May, 2016. IBC NLRD Identifier: 5201600395.

Patrick Alexander da Roza

October 2017

Acknowledgments

First, my sincerest gratitude to my supervisor Prof. Helena Nevalainen for the opportunity to undertake the research program under her supervision as well as my associate supervisors Dr. Angela Sun and Associate Prof. Anwar Sunna for endless support, wealth of knowledge and advice. Their doors were always open and without their input, encouragement and guidance, this work would not have been made possible.

Secondly, thank you to all my colleagues and lab members. To Dr. Hugh Goold, Bishal Khatiwada and Mafruha Hasan for their knowledge and help with *Euglena* and algal cultivation. To Dr. Liisa Kautto for her training and management of the laboratory. To Benjamin Ford, Dylan Russell, Stephanie Nagy, Raymond Wei Wern Chong, Edward Moh , Elizabeth Wightman, Alexander Gissibl, Wisam Babar, Dominic Logel, Vanessa Pirotta, Varsha Naidu and Elizabeth Daniel for their companionship and advice.

I would like to express my appreciation to the members of the Macquarie University Flow Cytometry Facility. In particular, to Dr. Martin Ostrowski who has been a mentor over the past two years and to Dr. Sasha Tetu and Amaranta Forcardi for their tutelage and use aid with instrumentation. Additionally, I would like to acknowledge the Macquarie University Microscopy Unit and Dr. Arthur Chien for aid with microscopy imaging.

I would also like to express my gratitude to my family and friends who have supported me throughout this research project and all my studies. Especially to my parents for their worldly advice and encouraging me to pursue goals and interests. Finally, a very special thank you to my wonderful partner Kimberley, whose continual love and support has filled each day will joy and has enabled me to meet the challenges that I've faced.

Sincerely,

Patrick

Abbreviations

Em	Emission wavelength
Ex	Excitation wavelength
DBM	Dry biomass
PBS	Phosphate buffered saline
PSA	Phenol-sulphuric acid
FCM	Flow cytometry
FSC-A	Forward scatter - Area
KO525-A	Emission band pass used for detection of aniline blue fluorophore. Ex 405 nm, Em 525/40 nm.
MFI	Median fluorescence intensity (arbitrary units)
PC5.5-A	Emission band pass used to detect chlorophyll fluorescence. Ex 561 nm, Em 690/50 nm.
PerCP-A	Emission band pass used to detect chlorophyll fluorescence. Ex 488 nm, Em 690/50 nm.
SSC-A	Side scatter – Area. FCM parameter used to detect cell granularity.

Chapter 1: Introduction

1.1 Microalgae in biotechnology

Microalgae are a biochemically diverse collection of photosynthetic unicellular microorganisms that can grow in freshwater and marine systems [1]. They are primary producers, converting sunlight, water and carbon dioxide into algal biomass. Over 15,000 novel compounds have been chemically determined from algal biomass [2], including bioactive compounds such as antibiotics, algaecides, toxins, and plant growth regulators [3-5]. Furthermore, microalgae can synthesise carbohydrates of various forms, polysaccharides and glucose sugars [6] and are valuable sources of essential fatty acids and vitamins such as A, B_1, B_2, B_{12}, C, E, biotin, nicotinate, pantothenic acid and folic acid [6-8]. Due to their ability to produce numerous valuable compounds, microalgae have been utilized in the production of human food, animal feed and aquaculture, pharmaceuticals, cosmetics, and biofuels [5, 9-14]. For example, Table 1 demonstrates that some microalgae have macro-nutritional profiles comparable or superior to conventional food sources. It has been estimated the total microalgal biomass market generates 5,000 tons of dry matter and has a turnover of $1.25 $\times 10^9$ (US) per year [15].

Table 1. Protein, carbohydrate and lipid content as a percentage of dry matter of various food sources and species of algae, from Becker [6].

Source	% Protein	% Carbohydrate	% Lipid
Aphanizomenon flos-aquae	62	23	3
Chlamydomonas reinhardtii	48	17	21
Chlorella vulgaris	51-58	12-17	14-22
Euglena gracilis	39-61	14-18	14-20
Egg	47	4	41
Meat	43	1	34
Milk	26	38	28
Rice	8	77	2

1.2 Enhancing production of microalgal compounds

Techniques for improving microalgal production have traditionally focused on modifying and improving cultivation conditions. In the course of enhancing cultivation, various production systems have been implemented, including open systems such as large shallow ponds and tanks, and closed systems such as closed plastic bag cultures and tubular photo-bioreactors [16]. Recently, genetic engineering tools have also been developed for a range of microalgae such as *Chlamydomonas*

reinhardtii and *Volvox carteri* [17, 18]. These may be paired with cultivation techniques to further the progress of algal biotechnology.

Genetic and metabolic engineering can be used to direct metabolic pathways towards optimal production of inherent products [19] and has been undertaken with various algae for the production of lipids, fatty acids and the generation of sustainable algal based biofuels [20-24]. Genetic transformation of microalgae can be achieved by permeabalising the cells with glass beads [25], electroporation [17] or biolistic bombardment with DNA coated gold or tungsten micro-particles [26]. Despite the progress made, successful transformation has only been achieved in a few algal species [19]. One such example is the microalga *Euglena gracilis*, which has been investigated as a potential platform for production of food (*Euglena* Co Ltd. 2017 - http://www.euglena.jp/en/) , biofuels [27] and nutraceuticals [13, 28]. While chloroplast transformation of *E. gracilis* has been successful [29], nuclear transformation has so far remained elusive.

1.3   *Euglena gracilis*: background and features

Euglena gracilis is a eukaryotic microalgal species of single celled flagellate protist with the ability to grow in a diverse range of environments and conditions [13, 30, 31]. Like plants and other microalgae, *E. gracilis* contains chlorophyll, enabling it to photosynthesise and thus survive phototrophically. Yet, it can also survive heterotrophically like animals in both the light and the dark [30]. Sequencing of expressed sequence tags (EST's) from *E. gracilis* by Ahmadinejad, et al. [32] has helped to uncover some of its genomic and evolutionary history. This research has uncovered that *E. gracilis* originates from both kinetoplastid and photoautotrophic ancestors, and that it has a chimeric amalgamation of genes inherited from a photoautotrophic endosymbiont and from a heterotrophic protozoan like host. *E. gracilis*, as well as other euglenoids are now considered to belong to the protist phylum Euglenazoa.

E. gracilis has a number of notable physical characteristics. The cells may take both an active (slimmer) form favoured by photoautotrophic conditions or quiescent (rounded) sluggish forms which have less distinct organelles [30]. Active forms tend to be elongated at around 50 by 15 µm and up to 100 µm long, whereas the quiescent type form spheres of approximately 20 µm. For taxis, the cells may move using both their flagellum and a 'euglenoid' movement by expanding and contracting their surface. These changes in shape are enabled by a highly flexible cell surface, which contains a helicoidally striated pellicle (orientated in parallel ridges and groves) supporting the cell membrane [30, 33, 34]. *E. gracilis* cells contain a nucleus, numerous vacuoles, lipid inclusions,

mitochondria, carbohydrate granules, a red eyespot and highly productive plastids [13, 30, 35]. The morphologies and organelles of *E. gracilis* including vacuoles, granules, chloroplasts and eyes spots can be seen in Figure 1.
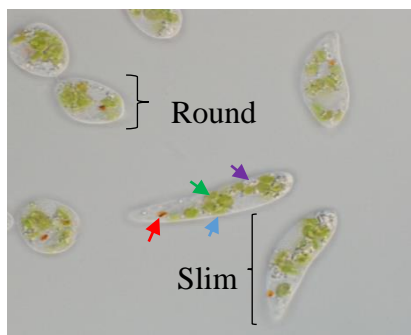
Figure 1. E. gracilis Z, displaying cells of both slim and round morphologies. Arrows indicate visible organelles: cell membrane with pellicle (blue), paramylon granules (purple), chloroplast (green) and stigmata/eyespot (red). Images taken by Mafruha Tasnin Hasan, Macquarie University, Department of Molecular sciences.

Furthermore, the biochemistry of *Euglena* may vary greatly depending on the wide range of growth conditions that it is capable of growing in (e.g. light vs dark and pH ranging from 3.0 – 9.0). *Euglena* has therefore been an ideal candidate for the investigation of light/dark adaptation in cells and the structure and chemistry of pigments and pigment containing organelles, such as chlorophyll and chloroplasts respectively [30, 36]. As a result, various species of *Euglena* including *E. gracilis* have been used extensively as model scientific organisms for biochemical and biophysical studies, leading to the investigation of a wide range of biological processes. These include photosynthesis and photoreception [30], chloroplast development [37], fatty acid biosynthesis [38], flagellar surface assembly [39], metal poisoning in eukaryotic cells [40] and mutagen and anti-mutagen screening [13]. *E. gracilis* has even been used to study gravitaxis and graviperception of cells during space flight [41]. However, for biotechnological applications, it is not its space faring adventures that are of interest, but its potential nutritional benefits.

1.4   Nutrition and valuable compounds from *Euglena*

E. gracilis is nutrient rich and contains high levels of antioxidants (e.g. α-tocopherol), vitamins, lipids, amino acids, glucans and essential fatty acids [13, 42, 43]. Furthermore, *E. gracilis* cells are efficient fixers of carbon dioxide and their photosynthetic productivity can be up to 60 times that of rice [44-47]. Due to this productivity, interest has been generated for the use *Euglena* (including *E. gracilis*) in commercial and industrial applications. This has been spearheaded by Tokyo based company 'Euglena Co Ltd' founded in 2005. They have cultivated the microalga in commercially viable quantities and have begun developing *Euglena* based food and beverage (human), feed (animal) and cosmetic products with a further outlook towards the application of *Euglena* for biofuel production and carbon capture (Euglena Co Ltd. 2017 - http://www.euglena.jp/en/).

In addition to the previously mentioned compounds, *E. gracilis* produces paramylon (a crystalline β-1,3-glucan) as a reserve polysaccharide [48, 49], which accumulate in intracellular granules of varying morphologies depending upon species and strain [50, 51]. These granules can be clearly seen within the cells as displayed by *E. gracilis* var. *saccharophila* in Figure 2.
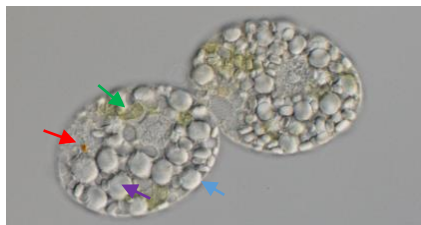
Figure 2. E. gracilis var. *saccharophila* containing numerous large paramylon granules as indicated by the purple arrow. Other arrow indicate the eyespot/stigmata (red), chloroplast (green) and cell membrane (blue).

Recent research has revealed paramylon to have several beneficial properties including involvement in the suppression of colon cancer [52], atopic treatment of skin lesions [53], suppression of HIV-activity [54] and hepatoprotection [55]. Furthermore, β-glucans are a potentially beneficial source of dietary fibre, moderating post-prandial blood glucose and insulin response [56] and having possible cholesterol lowing effects in humans [57]. Thus, having demonstrated activity as anti-infection and anti-tumour compound, paramylon has potential for therapeutic applications [58]. Due to these features paramylon is a potential commercially valuable compound and is of special interest in the current research.

1.5 Conditions for the synthesis and degradation of paramylon

Studies on the synthesis and degradation of paramylon in *E. gracilis* have primarily focused on investigation of cultivation conditions and have largely relied upon gravimetric and biochemical/colorimetric methods for quantification [28, 48, 59-61]. These studies have been successful in enhancing paramylon production, with quantities ranging from 50 – 90% of dry mass of *Euglena* depending on the strain, growth phase, primary carbon source and trophic conditions of the cultivation [28, 48, 60, 61]. In general, paramylon synthesis is improved by growth at relatively low temperatures (e.g. 15°C > 33°C) under heterotrophic conditions with a readily available carbon source such as glucose [28, 48, 62, 63], with the cellular content peaking during the late lag and early exponential growth phase of both light and dark grown cells [28]. Following synthesis, paramylon reserves are broken down with the onset of cell division and are greatly reduced once the stationary phase of cultivation is reached [28, 63]. At this stage, the activity of a probable paramylon degradation enzyme β-1,3 glucanase in the organism, has been reported to double [64]. Paramylon may also be converted to wax esters by transfer to anaerobic conditions [65-67].

4

1.6　Chlorophyll development and paramylon in *E. gracilis*

Euglena are highly efficient at fixing carbon and they contain both chlorophyll a and chlorophyll b, which they employ in the process of photosynthesis in the presence of light [30, 68]. Previous laboratory experiments and published literature have noted a relationship between chlorophyll production and paramylon degradation/utilisation in *E. gracilis.* In dark grown cells and carbon starved dark grown cells, paramylon (β-1,3-glucan) is either preserved or utilized at a highly diminished rate, but is rapidly broken down/utilized upon exposure to light [49, 69]. Additionally, the development of chloroplasts and their morphology appears to be connected to the paramylon synthesis and light-induced degradation. Kiss, et al. [63], found that when paramylon levels were high in *E. gracilis*, pyrenoids (a sub-cellular compartment of chloroplasts) were absent, and when the cell had a relatively low content of paramylon, the pyrenoids were present. Dwyer, et al. [69] also examined this relationship and found that the light-induced break down of β-1,3-glucan in *E. gracilis* was associated with the development of chloroplasts as a whole, but was not experienced by non-pigment producing bleached mutants. This suggests that photosynthesis and the metabolic state of the cells are linked to the production and or degradation of paramylon, and that paramylon could serve as a source of energy to survive periods of darkness, food scarcity, or for the synthesis of chlorophyll components when switching from heterotrophy to photoautotrophy [69, 70]. In the production of paramylon content in *E. gracilis,* the analysis of chlorophyll in the cultured cells would provide a useful insight into their metabolic state and act as a potential aid in avoiding rapid degradation of accumulated paramylon.

1.7　Enhancing paramylon production in *E. gracilis*

Alongside optimised cultivation conditions, enhancement of paramylon production in *Euglena* would benefit from the development of strains with improved production levels and efficiency. To this end, several viable options present themselves, such as the genetic modification of biosynthetic pathways and production of recombinant *Euglena* for overexpression of paramylon synthesis. While the sequencing of chloroplast DNA in *E. gracilis* has been undertaken [71], the nuclear genome sequence has not yet been completed. Sequencing of the nuclear genome would be greatly beneficial as it would allow the development of *Euglena* specific molecular tools and enable the genetic characterisation of highly productive *E. gracilis* strains. In the meantime, improved strains may be developed by production and screening of *E. gracilis* mutants. This for example has been undertaken by Yamada, et al. [27] who used Fe-ion irradiation in combination with fluorescence activated cell sorting (FACS) in the generation oil rich *E. gracilis*.

High-throughput screening via flow cytometry has been used for identifying and selection highly productive oil mutants in *E. gracilis*, *Nannochloropsis*, and *Chlamydomonas reinhardtii* [27, 72, 73]. However, flow cytometry screening for paramylon producing *E. gracilis* has not yet been accomplished. Instead, determination of paramylon content in *E. gracilis* is reliant on biochemical and gravimetric methods [36, 59, 74]. These methods are time consuming and do not have potential for live sorting and rapid strain development applications. Therefore, exploring the analysis of paramylon using fluorescence and flow cytometric methods with high-throughput capabilities and potential sorting applications would benefit the development and selection of high paramylon producing *E. gracilis* strains, variants and mutants.

1.8   Fluorescence as a biological tool: dyes and probes

With an array of fluorescent dyes and DNA-encoded markers now available, fluorescence has become widely utilised for the analysis of entire biological processes, specific cells, cellular components and molecules [75]. Fluorescent dyes, probes and markers contain fluorescent chemical compounds, which react with or bind to biological molecules and re-emit light of various wavelengths following excitation by a light source, thus enabling the examination of both fixed cells and the dynamic processes undertaken in live cells [76]. Fluorescent dyes and probes may also be paired with a range of detection methods such as fluorescence spectroscopic methods, fluorescence microscopy based techniques and flow cytometry [77-79].

Table 2. Common fluorescent dyes/probes and their targets.

Type/Target	Example fluorescent dye/probe	Reference
Cell viability	Fluorescein diacetate	[80]
Fluorescent proteins	Green fluorescent protein	[81]
Intracellular ions	Fura-2	[82] [83]
Lipids	BODIPY $^{505/515}$	[27]
Membranes	Dil (1,1'-Dioctadecyl-3,3,3',3'- Tetramethylindocarbocyanine Perchlorate ('DiI'; DiIC18(3))	[84]
Membrane potentials	Tetramethylrhodamine (TMRM)	[85]
Nucleic acids	SYTO RNASelect, PicoGreen	[86]
Oxidative activity	Dichlorodihydrofuorescein diacetate (H2DCFDA)	[87]

1.9   Characteristics of fluorescent dyes and probes

Several characteristics such as delivery, targeting, detectability and fluorescence response must be considered in the selection of fluorescent dyes and probes for their application to cellular systems [76]. For delivery, the fluorophore must be able to be introduced into the cell, cellular integrity should be maintained and for live staining, the cells should remain viable. The method of delivery may be

simple, for example, probes with lipophilic characteristics might only require the addition of water miscible stock solution [76]. However, larger and/or more polar probes may require the use of various methods to coax or force their uptake, such as the use of surfactants to increase cell membrane permeability [88]. In addition to delivery, fluorophores/fluorescent probes must also be able to selectively interact with their target, whether that be a type of structure or a specific organelle, molecule or ion. The fluorescence response of this interaction must then be strong enough to allow detection of the target [76], either by spectroscopic response (fluorescence intensity) or by spatial distribution (e.g. spectral shift). Lastly, the characteristics of the spectra also need to be compatible with the instrument doing the detection. For example, the instrument has to be equipped with the appropriate excitation source, filters and detectors [76]. Thus, when employing fluorescence as tool for biological investigation, the targets, fluorophores and instruments must be carefully matched.

1.10   Flow cytometry for microalgal biotechnology

Flow cytometry (FCM) is a technique which allows counting and examination of cells and other biological and non-biological particles. FCM is based on the quantification of scattered light emitted from cells as they pass through an excitation source (laser) in a hydrodynamically focused stream, and allows a high-throughput of over 10,000 cells/second [89]. FCM instruments may also be designed with sorting functions (cell or flow sorter) and combined with fluorescence detection in Fluorescence Activated Cell Sorting (FACS), thereby allowing the rapid analysis of populations and sorting of desired cells.

Flow cytometry has been applied to an extensive range of purposes, such as monitoring of T-lymphocytes during HIV infection, separation of sperm via sex chromosomes for animal breeding and chemical analysis of ligand binding to solid substrates and particles [79]. FCM methods have also been established for ecological studies of microalgae [90-92] and biotechnological processes (e.g. production of target compounds and growth condition optimisation) involving bacteria and yeasts [93-95]. FCM has previously been used to study various processes in *Euglena* such as cell cycle, growth, motility and cytotoxicity (Table 3).

Table 3. Example applications of flow cytometry for *Euglena.*

Focus	Target	Dye/probe	Reference
Cell cycle, growth response	Nucleic acid (DNA)	Ethidium bromide	[96] [97]
Cell growth and motility		Hoechst 32258	[98]
Cytotoxicity	Glycoprotein-lectin binding	FITC	[99]
Cell surface carbohydrates	Carbohydrates -lectin binding	N/A	[100]
Cell viability	Nucleic acid (DNA), Chloroplasts	Propidium iodide, Autofluorescence	[101]
Oil/lipid production	Intracellular lipids	BODIPY $^{505/515}$	[102]
Cell morphology		Label free	[103]
Species differentiation	Nucleic acid, Chloroplasts	Hoechst 33342, DAPI, auto-fluorescence	[104]

FCM can also be applied to the development and improvement of biotechnological processes and production in microalgae by allowing the counting, examination and sorting of cells. For example, cellular features such as cell viability, enzyme activity and chemical composition can be assessed and over-producers of a target compound and axenic cultures can be isolated [89]. A general FCM workflow outlined by Hyka, et al. [89] can be adapted here for the development of high-paramylon producing *E. gracilis* strains and variants (Figure 3). In this case, *E. gracilis* strains, mutants or recombinants could be first analysed and screened using a flow analyser to monitor and optimise the generation of paramylon. FCM analysis could additionally be paired with fluorescence activated cell sorting (FACS) for iterative selection overproducing cells to develop improved strains for industrial production.
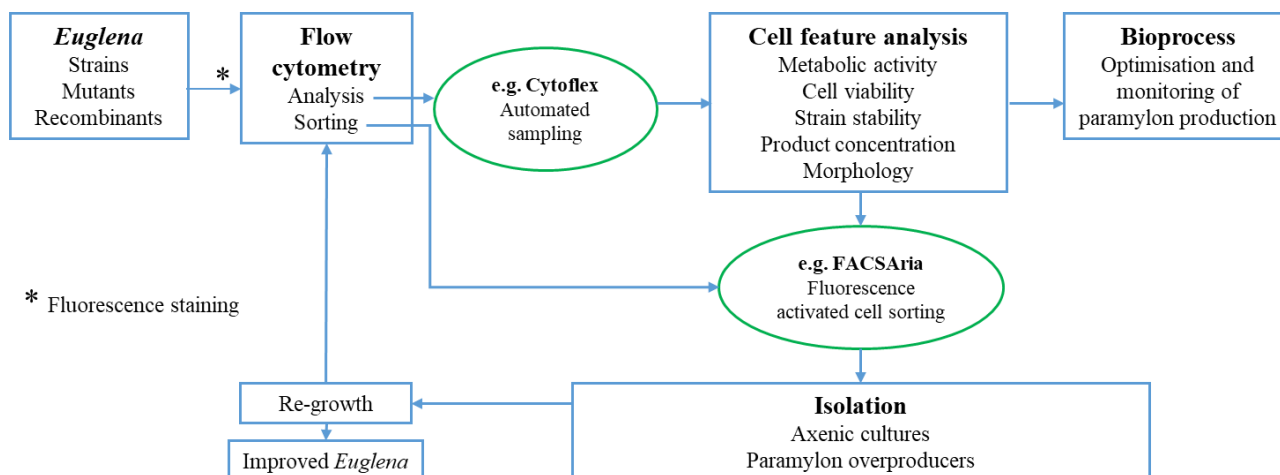
Figure 3. Possible applications of flow cytometry for the analysis and development of paramylon rich *E. gracilis* strains, as adapted from Hyka, et al. [89]. Applications and stages are contained in boxes and linked with arrows (blue). Instruments that could be applied to these applications are circled (green). The 'Cytoflex' (Beckman Coulter) is a flow analyser with available automated sampling configuration. The 'FACSAria' (BD Bioscience) is a flow sorter.

1.11   Determination of microalgal cell features

A wide range of cellular features may be examined using FCM. These can be monitored throughout cultivation of microalgae and implemented to determine the optimal conditions, species and strains for the development of the target products.

1.11.1 Morphology (size and granularity)

The two primary scatter signals detected in FCM are forward scatter (FSC) and side scatter (SSC) [79]. These two signals enable the examination of the morphology of microalgae which can be influenced by culture conditions, density and state of the cells. In general, FSC is proportional to the volume or size of a cells (signal intensity increases with the cell diameter or area) [105, 106]. SSC is effected by morphology, intracellular structures and complexity. In particular, SSC is usually associated with the level of intracellular granularity [94].

1.11.2 Pigment auto-fluorescence

Microalgae contain photosynthetic pigments, primarily composed of carotenoids and chlorophylls (and occasionally phycobilins) [89]. Pigmentation can depend on the taxa, species or strain of the microalga [107-109] and is largely responsible for the auto-fluorescence of microalgae [110]. Pigment fluorescence has been used in conjunction with FCM to assess photosynthetic capacity, identify cellular pigments and detect pigment rich species [111-113].

1.11.3 Biomass composition

The relative biomass composition of microalgae can vary largely depending on the species [10] and cultivation conditions such as pH, temperature, light and nutrients [28, 63, 114]. FCM is particularly useful for determining biomass composition as its high-throughput capabilities can be paired with a wide range of fluorescent dyes and probes which target specific compounds. Examples include, the analysis of lipids using fluorescent dyes such as nile red and BODIPY$^{505/515}$ [27, 115], protein and nucleic acids using the fluorescent dyes SYTO RNASelect, PicoGreen and fluorescein-5-ex-

succinimidylester [86], and carbohydrates (e.g. starch granules) using either SSC or the fluorescent dye calcofluor white M2R [116-118].

1.11.4 Cell viability

Assessing cellular viability is relevant for many research applications as well as biotechnology since only viable cells are involved with production and biomass growth. One way to assess cell viability employs the use of fluorescent stains in combination with either fluorescent microscopy or FCM [119]. The most common method is to assess the permeability/damage to cell membranes using nucleic acid dyes. While these are unable to stain undamaged cells, they will stain permeabalised cells and therefore give an indication of cellular damage [89, 120].

1.11.5 Enzyme activity

Enzymatic activities can provide physiological information on the state of live cells. Some of these such as phosphatase or esterase can be examined using FCM [89]. For example, esterase activity in microalgae may be examined using uncharged non-fluorescent fluorescein diacetate probes. Once the probes enter a cell, they are hydrolysed by enzymes to become fluorescent and polar. As a result, the probes are retained within the cell membrane and become fluorescent allowing examination of the activity of the target enzyme [121].

1.11.6 Cell sorting

Flow cytometry instruments may also be equipped with sorting capabilities, allowing high-throughput separation of cells according to their size and morphology (FSC and SSC) and their fluorescence (FACS). The most common implementation of this is droplet sorting as displayed Figure 4. Here, the flow stream containing the cells of interest passes through a vibrating nozzle and is subsequently fragmented into droplets each containing single cells. As the cells are detected, those that lie within a user defined 'gate' may be given a charge (+ or -). The droplets then pass through an electro-magnetic field and those that have been given a charge are deflected and collected into tubes, agar plates or a 96-well plate. They may then be used for further analysis or recovered for cultivation as required by the user [79].
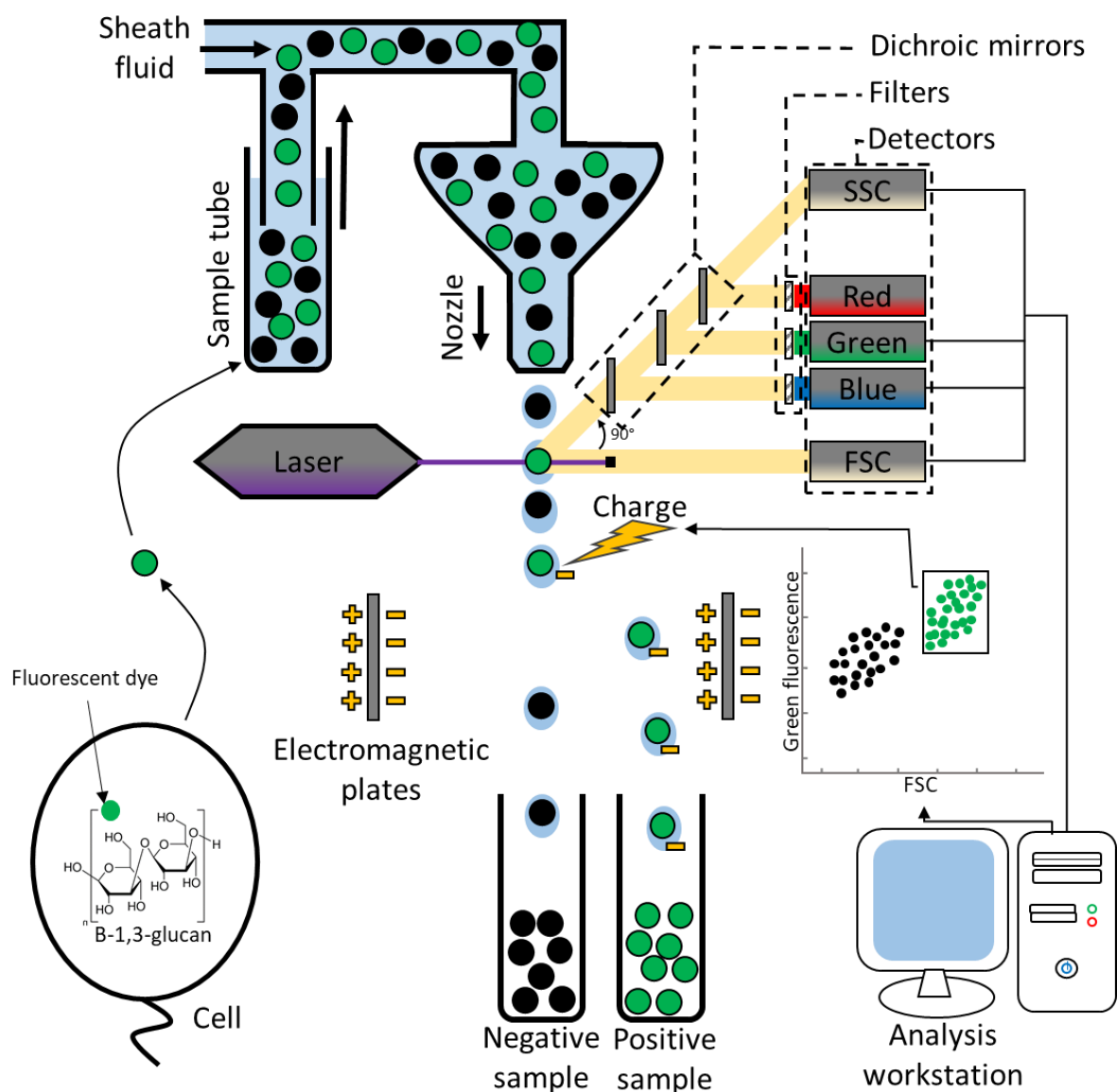
Figure 4. Schematic of fluorescence activated cell sorting for microalgal cells containing biotechnologically relevant compounds (e.g. β-1,3-glucans). Cells are stained with the relevant fluorescent dye and injected into the instrument sheath fluid. Cells are separated into single droplets and excited with a laser. Scattered light and fluorescence is emitted, and refracted using mirrors. Light is split into specific wavelengths using band pass emission filters and subsequently detected. Computer and software analysis is used to identify target cells by their scatter and fluorescence, and gate them for sorting/ isolation. The target cells are charged as they pass through electromagnetic plates, redirecting them into collection tubes or microplate wells. Non-target cells can be collected or sent to waste.

One common practice is to employ cell sorting for the preparation of axenic cultures. This feature is invaluable for cultivation of microalgae in heterotrophic conditions, which have an increased risk of overgrowth by contaminants (e.g. bacteria or fungi) [122]. For example, sorting using FACS has

previously been applied to the preparation of clonal and axenic cultures of various algae [122, 123] and in the isolation of uni-algal phytoplankton cultures from heterogeneous samples [124].

Furthermore, sorting may be utilised for the isolation of microalgal strains that exhibit improved features or overproduction of targeted compounds such as starch and lipids. This is advantageous as it provides additional support to the optimisation of cultivation conditions and selection of cells using tedious methods such as picking single cells via microscopy or growing and picking colonies from plates. Besides sorting for optimal strains under various cultivation conditions, cells with desired features (such as overproducers) can be screened and isolated after exposure to mutagens such as alkylating agents [125] or Fe-ion irradiation [27, 126]. This is especially valuable for working with *E. gracilis* in which nuclear transformation has so far been unsuccessful [89].

1.12   Fluorescence and scatter detection in *E. gracilis*: probing paramylon (β-1,3-glucan)

Despite the abundance and popularity of fluorescence based indicators starch and carbohydrate specific fluorescent dyes for microscopy and FCM are not widely available. In the absence of fluorescent dyes and probes, reserve polysaccharide content can be estimated from side/right angle scatter signal (SSC), where light that is scattered from the object/cell and subsequently detected at 90° from the incident light source. SSC can be used during flow cytometry as a measure of cell granularity and intracellular complexity, which in turn corresponds to the presence of intracellular polysaccharide granules such as paramylon [116]. SSC measurement does present a challenge for the detection of paramylon (β-1,3-glucan) content in *E. gracilis*, since other organelles and cell components can influence the intensity of this signal. However, in addition to SSC signal detection, there are two potential fluorophore candidates which may aid in fluorescence based detection and analysis of paramylon content.

The first of these candidates is a dye called 'aniline blue', otherwise known as 'water blue' or 'methyl blue'. Aniline blue is triaryl-methane dye containing a fluorochrome as minor component/impurity, which forms a fluorescent complex upon binding with β-1,3-glucans (e.g. paramylon and laminarin), β-1,4-glucans (e.g. cellulose) and some β-1,3/ β-1,4 mixed linked glucans (e.g. lichenan). While the fluorescence spectrum of aniline blue is slightly variable depending on the pH and target glucan, upon binding to paramylon, the fluorescent complex generally exhibits an excitation maximum of 395 nm (near UV/violet) and an emission maximum of 506 nm (green) [127, 128]. This dye has been used previously as a histological dye for glycan structures in plants [129, 130] and for the quantification of extracted β-1,3-glucans from various foods [131], but as yet has not been implemented in *Euglena*.

Since violet excitation lasers (405 nm) and matching filters are commonly available, examination of aniline blue fluorescence should be possible using both microscopy and FCM instruments, thus allowing fluorescence detection of paramylon in *E. gracilis* once labelling of the granules is achieved.

The second fluorescent dye is calcofluor white M2R, otherwise known as 'fluorescent brightener'. This dye has been shown to bind to a range of β-1,3 and β-1,4-glucans, but shows little affinity for most polysaccharides [132, 133]. Calcofluor white M2R has primarily been implemented for the staining of chitin and cellulose in plant and fungal cell walls [89, 134], but has also been used as vital stain in animal and plant cells [135].

One of the primary challenges in the use of these dyes, is that neither has been previously used for staining intracellular compartments or granules in euglenoids such as *E. gracilis*. These, unlike plant cells and many other algae, contain a protein rich pellicle supporting the cellular membrane rather than a cell wall constructed of cellulose [33, 34, 136]. Consequently, the capability of either of these dyes to fluorescently stain intracellular paramylon in *E. gracilis* is unknown and must first be investigated.

1.13 Fluorescence and scatter detection in *E. gracilis*: chlorophyll development

Traditionally, quantification of chlorophyll content has been undertaken using either spectrophotometric or colorimetric methods [68, 137]. Yet, due to bright red fluorescence emitted by chlorophylls upon excitation with blue to red light, determination of chlorophyll content can be achieved using fluorescence based methods [138]. For example, flow cytometry chlorophyll analysis has be used distinguish species of phytoplankton and algae, cell debris and non-photosynthetic bacteria [111]. Additionally, it has been used for quantification of photosynthetic capacity/activity, identification of cellular pigments [111, 112] and examination of cell cycle progression [139].

The ability to assess chlorophyll content with FCM in *E. gracilis* offers a range of potential benefits towards continuing improvement of cultivation conditions and strains for paramylon production. It could prove useful for distinguishing different strains and mutants, and for excluding those that have an overly fast rate of chlorophyll production that could result in early degradation of paramylon reserves. In addition, characterisation of chlorophyll fluorescence in *E. gracilis* could also serve as an additional parameter for future sorting of strains and preparation of axenic cultures.

1.14   Aims of the study

Microalgae constitute a broad collection of unicellular photosynthetic microorganisms that are now playing an ever-greater role in biotechnology and industrial production. Biochemically diverse, microalgae have high potential as a nutritious source of food and are used in the production of many valuable compounds. *E. gracilis* has only recently attracted attention as a viable organism for commercial applications. Of interest is the β-1,3-glucan paramylon which *E. gracilis* accumulates as a reserve polysaccharide and has been found to have medically and nutritionally beneficial properties. While the gravimetric and colorimetric methods currently employed for quantification are reliable and have been widely used, they are time consuming and can only be applied to low throughput applications. To further improve production of paramylon in *E. gracilis*, efficient monitoring of cultivation conditions and metabolic state, and selection of highly-productive strains will be required. This task will require the establishment of high-throughput analysis capabilities to screen thousands of cells at a time.

The overall goal of this work was to investigate the use of fluorescence and flow cytometry based methods for the detection and analysis of paramylon and chlorophyll in *E. gracilis*. This would allow future high-throughput screening of desirable strains and culture conditions with enhanced paramylon production and enable efficient monitoring of the metabolic state of the cells. Specifically, this work aimed to:

- Develop a fluorescent staining method for the intracellular paramylon in *E. gracilis*, to be assessed via fluorescence and confocal microscopy.
- Validate use of flow cytometry for paramylon and chlorophyll analysis in *E. gracilis*.
- Investigate use of flow cytometry to monitor paramylon content and chlorophyll development during the cultivation.

Chapter 2: Materials and methods

2.1   *Euglena gracilis* strains, culture medium and cultivation conditions

Euglena gracilis Z (UTEX 753) and *Euglena gracilis* var. *saccharophila* (UTEX 752) were obtained from the UTEX Culture Collection of Algae, The University of Texas at Austin (F0402) Austin, TX 78712 USA. An additional variant, *E. gracilis Zm*, was also examined. This variant was previously produced in house by cultivating the *Z* strain under dark heterotrophic conditions until chloroplasts were absent.

Euglena gracilis strains were cultured using a modified medium by Rodríguez-Zavala, et al. [59] based on an original cultivation recipe by Hutner, et al. [140]. Per 1 L of total medium, the salt and mineral base contained 0.2 g of $CaCO_3$, 0.5 g of $MgSO_4$, 0.4 g of $(NH_4)_2HPO_4$, 0.2 g of KH_2PO_4, 1.81 g of NH_4Cl, 10 g of yeast extract (total 1%) as a source of nitrogen, 2 ml of mineral stock A (4.4 g $ZnSO_4·7H_2O$, 4 g $MnSO_4·4H_2O$, 1 g $Na_2MoO_4·2H_2O$ and 0.08 g $CoCl_2·6H_2O$ per 100 ml ddH_2O), 1 ml of mineral stock B (0.078 g $CuSO_45H_2$ and 0.057 g H_3BO_3 per 100 ml ddH_2O) and 898.4 ml ddH_2O. The pH was adjusted to 3.5 to inhibit bacterial growth, followed by sterilisation at $121°C$ for 20 min. Medium was left to cool to room temperature before the addition of 88.5 ml of 20% (w/v) glucose per litre (a total of 1.77% (w/v) glucose per litre, sterilised separately at $121°C$ for 20 min), 1 ml of Vitamin B_1 stock (10 mg per ml of ddH_2O, filter sterilised at 0.22 µm) and 0.1 ml of Vitamin B_{12} stock (5 mg per ml of ddH_2O, filter sterilised at 0.22µm). Medium was stored at $4°C$.

Next, 250 ml Erlenmeyer flaks were capped with filter paper and sterilised at $121°C$ for 20 min then dried overnight at $70°C$. To cultivate *E. gracilis* strains, culture medium was transferred to the 250ml Erlenmeyer flasks and approximately 6.0×10^7 cells (as determined by hemocytometer count) were then transferred to the flasks per 50 ml of *Euglena* medium, unless stated otherwise. All *E. gracilis* cultures were grown under mixotrophic/photoheterotrophic conditions, receiving both sun-light with a natural day/night cycle and glucose as a carbon source. *E. gracilis* cultures were incubated at $23°C$ with continuous shaking at 150 rpm. Cells were maintained by subculturing 1.2×10^6 cells/ml of the parent cultures in a fresh medium.

2.2   Cell count

Estimation of the cell count for *E. gracilis* cultures was conducted using an Olympus BH-2 microscopy and a 'Neubauer improved bright-line' hemocytometer slide. Cells were harvested via pipette and serial dilutions of 1/10, 1/100 and or 1/1000 were prepared as necessary using ddH_2O. A clean coverslip was then placed on the slide and 10 µl of the cell dilution was pipetted into the slide through the notched wells. Cells were viewed using the microscope and counted on the hemocytometer grid. Cell concentration was calculated as per manufacturer instructions in cells/ml.

2.3   Fluorescence spectrophotometry

Fluorescence spectrophotometry was undertaken for three strains of *Euglena gracilis*: *Z, Zm* and var. *saccharophila*. Spectrophotometry was conducted in order to determine the auto-fluorescence spectra of the cells to ensure that the auto-florescence would not conflict with the fluorescent dyes during microscopy and flow cytometry. Approximately 6.0×10^7 cells of each *E. gracilis* strain were

cultivated in 50 ml of the *Euglena* medium in triplicate under the conditions described in section 2.1. Two ml samples were harvested from the cultures on day 2 (48 h post inoculation) and day 8 (192 h) of cultivation to assess if the auto-fluorescence spectra would vary greatly within a full cultivation period. Cells were centrifuged at 600 g for 2 min and the supernatant was discarded. The pelleted cells were then washed in 2 ml of medium by centrifugation at 600 g for 2 min and re-suspended in 2 ml of medium. A cell count was conducted using a hemocytometer. Auto-fluorescence of the cells was measured using a 'Cary Eclipse Fluorescence Spectrophotometer' (Agilent Technologies). Approximately 2×10^6 cells/ml were pipetted into UV/VIS spectroscopy cuvette (PerkinElmer). The spectrophotometer readings were blanked with cultivation medium and emission (Em) spectra were taken for common fluorescence excitations (Ex) for all replicates and both cultivation days. Emission spectra included: Ex405 nm (Em410 – 750 nm), Ex488 nm (Em500 – 750 nm) and Ex635 nm (Em640 – 750 nm). Both Ex and Em slit widths were set to 5 nm.

2.4 Biochemical quantification of dry biomass and paramylon

The methods described below were used for quantifying dry biomass and paramylon content to which the fluorescence based microscopy and flow cytometry measurements of paramylon were compared.

2.4.1 Dry biomass determination

To determine the total dry biomass of *E. gracilis* cultures, aluminium weighing boats were labelled and dried at 70°C for a minimum of 2 h and then weighed. Three ml of cells from the cultures were harvested under aseptic conditions and centrifuged at 14,000 g for 10 min and the supernatant was discarded. Cell pellets were washed in 1 ml of ddH$_2$O, centrifuged at 14000 g for 10 min and supernatant was discarded. The pellets were then resuspended in 1 ml of ddH$_2$O and transferred to aluminium weigh boats. These samples were dried at 70°C in a drying oven for 72 h and weighed. To obtain the final dry biomass of the 3 ml of cells in g/L the following equation was used: dry biomass = (mass x 1000) ⁄ 3.

2.4.2 Biochemical quantification of paramylon (β-1,3-glucan)

The phenol-sulphuric acid hydrolysis (PSA) assay for the determination of sugars and carbohydrates [141] was used for the quantification of paramylon content in *E. gracilis* as implemented by Rodríguez-Zavala, et al. [59]. One ml of cell cultures was harvested and centrifuged at 14,000 g for 10 min at room temperature and the supernatant was discarded. Cell pellets were resuspended in 0.9 ml of ddH$_2$O followed by the addition of 0.1 ml of ice-cold 30% HClO$_4$ (Perchloric acid). Cells were vortexed for 1 min, centrifuged at 1,100 g for 2 min at room temperature and supernatant was

discarded. Pellets were resuspended in 1 ml of 1% Sodium dodecyl sulphate, vortexed for 1 min and boiled in water for 15 min, then centrifuged at 1,100 g for 15 min and supernatant was discarded. Pellets were then resuspended in 1 ml of 1 N NaOH. Fifty µl of each sample was transferred to a fresh tube alongside a set of 8 glucose standards prepared in 1 N NaOH, ranging from 0 – 3 mg/ml, followed by the addition of 0.6 ml of 5% (w/v) phenol and 1.25 ml of concentrated sulphuric acid (H_2SO_4). Tubes were briefly vortexed and incubated at 70°C for 30 min. Samples and glucose standards were then pipetted into 96 well plates in triplicates (200 µl per well) and absorbance was measured at 480 nm. Absorbance values from the sample wells were then plotted against a glucose standard curve to calculate paramylon concentration g/L. Paramylon content of *E. gracilis* cultures were then calculated as a fraction of their dry biomass.

2.5 Fluorescent staining of paramylon

Following fluorescence spectrophotometry in section 2.3, the initial phase of the project consisted of an investigation into the fluorescence staining of paramylon in *E. gracilis*. Two dyes, aniline blue (methyl blue– Sigma-Aldrich [M6900]) and calcofluor white M2R (Fluorescent Brightener 28 – Sigma-Aldrich [F3543]) were trialled for fluorescent staining of paramylon in *E. gracilis*. Fluorescence emission was assessed visually using an Olympus BX63 fluorescence microscope (330 – 385 nm excitation band pass filter, a DM 400 beam splitter, and a 420 nm emission long pass). A range of protocols and conditions were tested to introduce the dye into the cells and stain the intracellular paramylon granules. This included adaptations of methods from Brundrett, et al. [130], Ko, et al. [131], Hughes, et al. [134], Herburger, et al. [142], Uniacke, et al. [143], Jamur, et al. [144], Smith, et al. [145], Ogawa, et al. [146], Rasconi, et al. [147]. The use of chemical fixative agents was however avoided when staining to minimize the addition of chemical fluorescence, alteration of scatter signal and disruption of the cells during flow cytometry. The range of conditions examined for aniline blue and calcofluor white M2R staining of *E. gracilis Z* and *E. gracilis* var. *saccharophila* is listed in Table 4 and Table 5 respectively. It should be noted that not every combination of variable was trialled. For example, not all staining times and temperatures were trialled for all dye concentrations, buffer and permeabalisation methods.

Table 4. Staining conditions examined for aniline blue labelling of paramylon in *E. gracilis*.

Dye conc. (w/v)	Buffer	Permeabilisation method	Staining time and temperature
1.0% 0.1% 0.01%	Sorensen phosphate buffer (0.1M, pH 8.0) ddH2O *Euglena* Medium 0.5M NaCl and 0.05M NaOH in ddH2O 40 volumes ddH2O, 21 volumes 1M HCl and 59 volumes 1M glycine/NaOH buffer (pH 9.4) 2% Dimethyl sulfoxide 50% dimethyl sulfoxide 1x Phosphate buffered saline, 1M NaOH (pH 10, 10.4 and 11.0)	0.1% Saponin from quillaja bark 0.1% Tween 20 0.1% Triton x-100 10% v/v glycerol 50% (w/v) Polyethylene glycol and 1M Lithium acetate Electroporation: 1.2kV, 25µ, ∞ resistance, exponential decay in ddH2O 100% Methanol at -20°C	23°C for 1 h. 38°C for 20 min, 23°C for 30 min. 39°C for 20 min, 23°C for 30 min. 45°C for 20 min, 23°C for 30 min. 50°C for 20 min, 23°C for 30 min.

Table 5. Staining conditions examined for calcofluor white M2R labelling of paramylon in *E. gracilis*.

Dye conc. (w/v)	Buffer	Permeabilisation method	Staining time and temperature
0.1% 0.05% 0.01% 0.005% 0.001% 0.0005%	1x Phosphate buffered saline, 1M NaOH (pH 10) ddH2O 5mM NaOH, 50mM NaCl in ddH2O	0.1% Saponin from quillaja bark 0.1% Triton x-100	23°C for 15 min. 38°C for 10 min, 23°C for 20 min.

2.6   Fluorescence microscopy of *E. gracilis* and comparison to known paramylon content

Quantification of paramylon content alongside fluorescent staining and fluorescence microscopy of intracellular paramylon granules in *E. gracilis Z* and var. *saccharophila* was undertaken in order to assess the effectiveness of fluorescence detection and suitability for FCM analysis. Fluorescent labelling and microscopy was not conducted for *E. gracilis Zm* since its cellular auto-fluorescence most likely would have interfered with the emission signal of the dye/fluorophore used. The cells were not fixed to slides as the staining method was to be applied to live cells in solution for FCM.

2.6.1 Cultivation of *E. gracilis*, and quantification of paramylon and dry biomass

Approximately 6.0 x 10^7 cells of *E. gracilis* Z and var. *saccharophila* were inoculated in 50 ml of *Euglena* medium with glucose and cultivated as per section 2.1 in triplicate. Six ml of cells were then harvested from each culture on day 3 (72 h) and day 6 (144 h) after inoculation. Three ml was taken from each culture and used for dry biomass determination (see section 2.4.1). One ml of each sample was stored at -20°C and then later thawed in a water bath at 35°C for 10 min and used to determine paramylon content (see section 2.4.2).

2.6.2 Fluorescence staining of intracellular paramylon in *E. gracilis*

Staining and microscopy were undertaken on freshly harvested cells from both day 3 (72 h) and day 6 cultures (144 h). Unstained cells were used as a negative control and β-1,3-glucan from *E. gracilis* (Sigma-Aldrich 89862-5g-F) was used as both a stained positive control and unstained negative control. Two hundred and fifty µl of the harvested cells were aliquoted into 2 ml microcentrifuge tubes and washed with 1 ml of 1x phosphate buffered saline (PBS). Cells were centrifuged for at 600 g for 2 min, supernatant was removed and cells were washed once in 0.1 % (w/v) Triton X-100 for 15 min at room temperature. The permeabalised cells were then washed once in 1x PBS and resuspended in 1 ml of aniline blue solution (0.1% methyl blue [w/v] in 1x PBS, adjusted to pH 10.4 with NaOH and left overnight at room temperature to de-colorize). The cells were incubated in a water bath at 39°C for 20 min (in dark) and then left to stain for a further 30 min at 23°C in the dark with gentle shaking (150 rpm). Cells were then centrifuged for at 600 g for 2 min, supernatant discarded, washed 4 times for 5 min in 1x PBS and then resuspended in 250 µl of 1x PBS.

2.6.3 Fluorescence imaging

Eight µl of the stained cells and unstained controls cells and 0.01 g of stained and unstained β-1,3-glucan granules, were mounted on glass microscopy slides and imaged using an Olympus BX63 automated fluorescence microscope. Fluorescence microscopy was undertaken using a 330 – 385 nm excitation band pass filter (BP), a DM 400 beam splitter, and a 420 nm emission long pass. Operation of the instrument and imaging of cells was conducted using Olympus CellSens software. Contrast and brightness of images were adjusted with Fiji ImageJ software package [148, 149].

2.7 Confocal microscopy of fluorescently stained paramylon granules in *E. gracilis*.

2.7.1 Staining procedure for confocal imaging

Confocal microscopy was used to attain improved images of the aniline blue stained paramylon granules. The method for staining was the same as carried out for fluorescence microscopy and FCM

but also included an additional fixation (paraformaldehyde) and permeabalisation step (methanol). Approximately 6.0 x 10^7 *E. gracilis Z and E. gracilis* var. *saccharophila* cells were inoculated in 50 ml of *Euglena* medium without glucose and cultivated as described in section 2.1. Three days (72 h) after inoculation, 4.425 ml of 20% glucose was added to each culture, for a total 1.77% (w/v) glucose in the cultivation medium. Two ml were harvested from each cell culture 26 h after the addition of glucose.

After cultivation and harvesting, *E. gracilis* cells were fixed, bleached and stained with aniline blue. Samples were centrifuged for 2 min at 600 g, supernatant was removed and the cells were resuspended and fixed in 2 ml of 4 % (w/v) freshly prepared paraformaldehyde for 15 min. Two hundred and fifty µl of the cells were then washed once in 1x PBS and twice in 100% methanol (pre-chilled to -20°C) for 10 min at -20°C to aid fixation, permeabalisation and removal chlorophyll, and were then washed in twice in 1x PBS. Cells were centrifuged at 600 g for 2 min, supernatant discarded and the pellet was then washed in 0.1% (v/v) Triton X-100 for 15 min at room temperature, washed once in 1x PBS and resuspended in 1 ml of aniline blue solution as previously described. Cells were then incubated in a water bath at 39°C for 20 min in the dark and left to stain for a further 30 min at 23°C in the dark with gentle shaking at 150 rpm. Cells were then centrifuged, supernatant discarded and pellets washed 4x for 5 min in 1x PBS at pH 10.0 to prevent re-colorization of dye for improved imaging. For imaging, cells were resuspended in 1x PBS at pH 10, and 8 µl of the stained cells were mounted on glass microscopy slides and stored briefly in the dark before imaging. A simplified flow chart of the cultivation, staining and imaging procedure is shown in Figure 5.
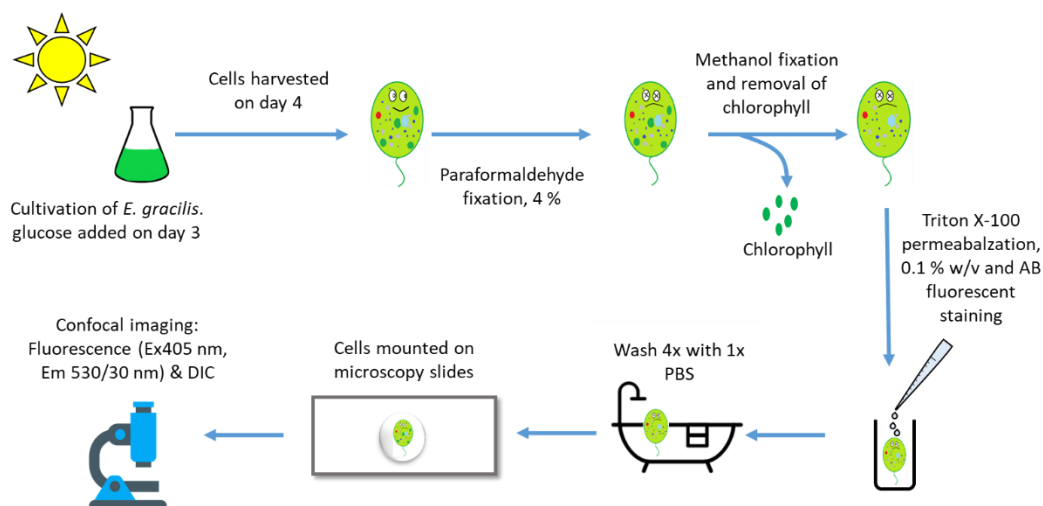

Figure 5. Simplified diagram of the mixotrophic cultivation, staining and confocal imaging of *E. gracilis Z* and *E. gracilis* var. *saccharophila*. Cells were stained with aniline blue (AB) and imaged using an Olympus Fluoview FV1000 IX81 Inverted Confocal Microscope using both fluorescence (Excitation 405 nm and Emission 530/30 nm) and differential interference contrast (DIC) modes.

2.7.2 Confocal imaging

Imaging was undertaken using an Olympus Fluoview FV1000 IX81 Inverted Confocal Microscope equipped with four laser diodes (405, 473, 559 and 635). Images were taken using the 405 nm (1.0%) excitation fluorescence channel with a 530/30 emission BP (PMT detector = 625 V, gain = 1.0, and offset = 9%) and the differential interference contrast (DIC) channel. Cells were viewed and imaged using a 60x objective, with a numerical aperture of 1.2 and scanning speed of 12.5 µs/pixel. Images were processed using the Fiji ImageJ software package [148, 149] to apply background subtraction (rolling ball radius = 10 pixels), gaussian blur smoothing (Sigma [radius] = 1.00) to the Ex405-Em530/30BP channel, to merge the fluorescence and DIC channels and for addition of scale bars.

2.8 Flow cytometry analysis of paramylon and chlorophyll in *E. gracilis*

2.8.1 Cultivation of *E. gracilis*

One hundred ml of *Euglena* medium in 250 ml Erlenmeyer flasks were inoculated with approximately 1.2×10^7 cells of *E. gracilis Z* and *E. gracilis* var. *saccharophila* in biological triplicates (total of 6 cultures) and cultivated as per section 2.1. Seven ml from each culture were harvested aseptically into 15 ml centrifuge tubes from each of the cultures 17 h after inoculation (overnight) and then at 24 h time points further 5 days (6 sample times/day and 42 ml each). Following sampling, aliquots were taken for paramylon quantification using the PSA assay (1 ml), measurement of dry biomass (3 ml) chlorophyll content (0.5 ml) and FCM analysis (0.5 ml), with 2.0 ml spare for any additional test required.

2.8.2 Paramylon and dry biomass quantification

If not processed immediately, the cells aliquoted for quantification of paramylon content, were frozen and preserved at -20°C. Frozen cells were thawed in a water bath at 35°C for 10 min before processing. Quantification of paramylon content was carried out using the PSA assay as per section 2.4.2. Cells for dry biomass determination were stored briefly at 4°C and then processed on the same day they were harvested from the cultures as described in section 2.4.1.

2.8.3 Spectrophotometric determination of chlorophyll content

The extraction and spectrophotometric determination of chlorophyll content was undertaken on the same day as samples were harvested. This was carried out as a measure of chlorophyll content against which chlorophyll analysis by flow cytometry could be validated. Samples were stored briefly at 4°C for no more than 1 h before the extraction and assay was carried out. Cells were first centrifuged at 600 g for 2 min and the supernatant was discarded. The pellet was resuspended in 1 ml of 90 % (v/v)

acetone, vortexed for 30 sec and incubated on ice for 30 min. Cells were re-vortexed for 30 sec and centrifuged at 2,000 g to sediment the solid matter, while extracted chlorophyll remained suspended in the solution. Two hundred and fifty µl of the supernatant from each sample were pipetted into a flat bottomed 96-well plate in technical triplicates. Ninety percent acetone was used as a blank for the readings and absorbance of the supernatant was taken at 647 nm and 664 nm using a BMG Labtech PHERAstar FS microplate reader. Chlorophyll concentration in *E. gracilis* was calculated using the absorbance readings according to the equation for chlorophyll a and b (per ml) in higher plants and green algae from Jeffrey, et al. [137]: chlorophyll a = 11.93 E_{664} - 1.93 E_{647}, chlorophyll b = 20.36 E_{647} - 5.50 E_{664} .The calculated concentrations were then adjusted for sample volume of 0.5 ml.

2.8.4   Fluorescent staining and sample conditions used for flow cytometry analysis

Three conditions were applied to *E. gracilis Z* and *E. gracilis* var. *saccharophila* cells for flow cytometry analysis: a) fluorescently labelled cells, b) unstained control cells, and c) bleached control cells (chlorophyll removed). All samples were analysed via FCM within 6 h of harvesting from their respective cultures on each day of analysis.

a) Fluorescently labelled cells: Two hundred and fifty µl of cells were aliquoted into 2 ml microcentrifuge tubes and stained using aniline blue as described in section 2.6.2. For day 1 (17 hours) samples, 250 µl of undiluted were pipetted into a 96-well flat-bottomed microplate due to a low cell count. For days 2 – 6, 25 µl of cells and 225 µl of 1x PBS (1:10 dilution) were pipetted into the microplate due to a higher FCM event rate (cell count).

b) Unstained control cells: Two hundred and fifty µl of cells was aliquoted into 2 ml microcentrifuge tubes and washed with 1 ml of 1x PBS. The cell pellets were centrifuged at 600 g and the supernatant was removed. Cells were washed a further 3x in 1x PBS in this manner. Cells sample were resuspended 250 µl of 1x PBS and pipetted in the 96-well flat-bottom plate in the same volume and dilution as the fluorescently labelled cells.

c) Bleached control cells (chlorophyll removed): Cells previously treated with 90% acetone in section 2.8.3 were retained as chlorophyll-less bleached controls and were used as a baseline for measurement of chlorophyll fluorescence intensity via FCM. These cells were re-centrifuged at 600 g for 2 min and remaining supernatant was discarded. To ensure all chlorophyll was removed, the cell pellet was then washed a further 2x in 90% acetone for 15 min each on ice, centrifuged 600 g for 2 min and the supernatant was discarded. Cells were resuspended in 1 ml of 1x PBS, washed for 5 min, centrifuged

at 600 g for 2 min and supernatant was discarded. The cells were washed a further 3x in the same manner and resuspended in 500 µl of 1x PBS and placed under ultra violet light in a biosafety cabinet for 25 min. Cells from all samples were aliquoted into the 96-well flat-bottom microplate for FCM analysis in the same volumes and dilutions as the fluorescently labelled cells (a) and the unstained control cells (b).

2.8.5 Flow cytometry of *E. gracilis*

Fluorescently labelled, unstained and bleached *E. gracilis Z and* var. *saccharophila* cells were analysed using a Beckman Coulter CytoFLEX S flow cytometer across 6 days of sampling in biological triplicates (total of 108 samples). The CytoFLEX S FCM instrument was equipped with a violet (405 nm, 80 mW), a blue (488 nm, 50 mW) and a yellow (561 nm, 30 mW) laser for generation of scattered light and fluorescence. Axial Light Loss sensor system using silicon photodiodes was equipped for forward scatter (FSC - 488/8 µm band pass filter) detection and Avalanche Photo Diode detector arrays for side scatter (SSC) and fluorescence detection were also available. CytExpert (2.0) software was used to run the instrument, the QC (using 'CytoFLEX Daily QC Fluorophores) and set acquisition settings and instrument gain as displayed in Table 6. The voltage pulse was identified using area of the peak for all parameters, for example, forward-scatter-area (FSC-A) and side-scatter-area (SSC-A). These settings remained constant across recording of all samples.

Table 6. CytoFLEX S acquisition settings for flow cytometry analysis of *E. gracilis*.

Laser (excitation wavelength)	Scatter/ emission band pass (BP) parameters	Target	Gain
Violet (405 nm)	KO525-A (525/40 nm)	Labelled fluorescence (paramylon)	110
Blue (488 nm)	FSC-A (488/8 µm)	Size, primary scatter detector	30
Blue (488 nm)	SSC-A	Granularity (paramylon)	25
Blue (488 nm)	PerCP-A (690/50 nm)	Red fluorescence (chlorophyll)	45
Yellow (561 nm)	PC5.5-A (690/50 nm)	Red fluorescence (chlorophyll)	300

An automatic FSC threshold was set using the CytExpert 2.0 software to eliminate noise and small debris/particles. Arbitrary units of 'fluorescence intensity' were used to measure emitted light scatter and fluorescence for 10,000 events per sample. The KO525 parameter was used to asses labelled paramylon fluorescence in stained cells, FSC for primary scatter detection in all conditions, SSC for

granularity (as a measure of paramylon content), and PerCP and PC5.5 as measures of chlorophyll fluorescence in unstained-control cells and bleached-control cells (baseline measurement).

2.8.6 Analysis of flow cytometry results

Analysis of FCM fluorescence intensity data was undertaken using 'Kaluza Flow Cytometry Analysis Software' (Version 1.5 - Beckman Coulter). From initial observation of FSC and SSC scatterplots of the data, two main populations were identified. These populations were defined based on FSC and SSC readings (gated) and labelled 'A' (high FSC and SSC population) and 'B' (low FSC and SSC population) as displayed in Figure 6. As displayed in Table 7 for the control cells, events in gate 'A' made up the majority of events, while those in gate 'B' the minority. Upon staining, a large percentage increase was seen in number of events in gate 'B'. The only difference between the control and stained cells was application of the staining treatment. It seems likely that the percentage increase in 'B' was due to the treatment, which suggested that events in 'B' were either free granules or other debris. Since intact cells were the events of interest in this work, analysis of relative paramylon and chlorophyll content was undertaken using median fluorescence intensity (MFI – arbitrary units) of population 'A' and not population 'B'.
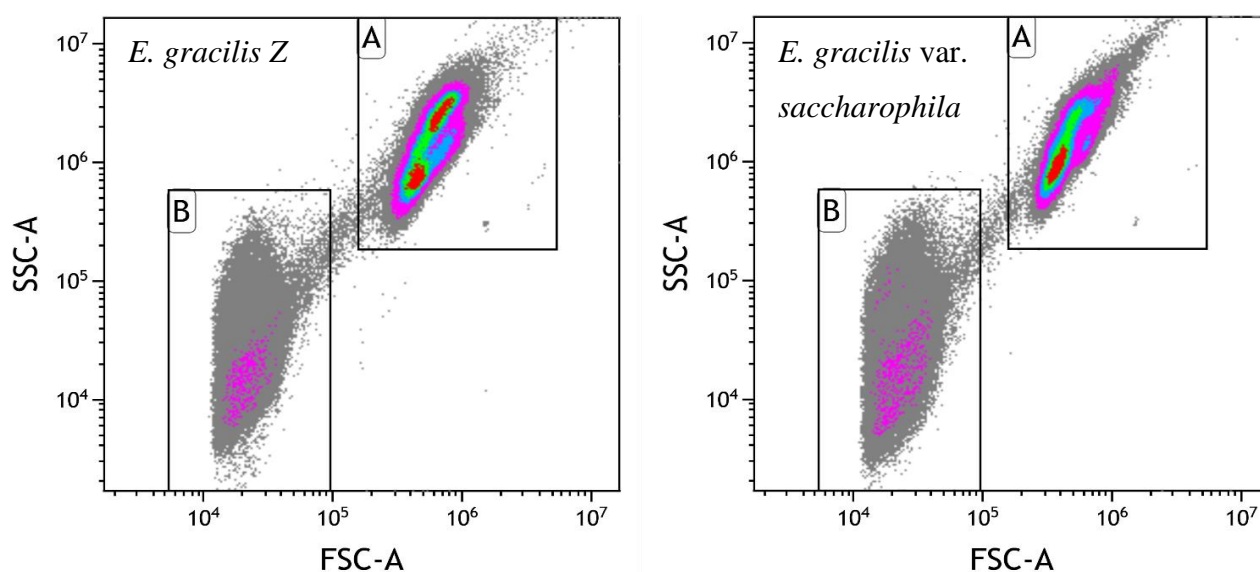
Figure 6. Density scatter plot displaying population gating of 18 merged unstained *E. gracilis Z* and *E. gracilis* var. *saccharophila* samples with a total 180,000 events each. Each plot contains forward scatter area (FSC-A) and side scatter area (SSC-A). Density is displayed by colour in order of lowest to highest: grey, pink, blue, green, and red. The high density population was designated 'A'. The lower density population was designated 'B'.

Table 7. Percentage of total merged events for FCM gates 'A' and 'B' of stained/labelled and unstained (control) *E. gracilis* Z and *E. gracilis* var. *saccharophila*.

Strain and staining condition	Gate [A] %	Gate [B] %
E. gracilis Z merged - unstained	80.35	19.34
E. gracilis var. *saccharophila* merged - unstained	78.30	21.45
E. gracilis Z merged - stained	44.95	54.65
E. gracilis var. *saccharophila* merged - stained	47.06	52.62

2.8.6.1 Analysis of paramylon content

To account for blue auto-fluorescence from *E. gracilis* in the detection of aniline blue florescence emission (KO525 - 525/40BP), median fluorescence intensity (MFI) of each unstained sample was used to compensate MFI of their corresponding stained cells. Pearson's correlation was then applied to compare MFI detected by for the 'A' population for the flow cytometry parameters KO525, SSC (stained and unstained cells), FSC (stained and unstained cells) against paramylon per dry biomass from the PSA assay. Statistical analysis in all sections was undertaken using GraphPad Prism 7 software (GraphPad Software, Inc. 2017). MFI of KO525, SSC and the PSA assay were also averaged between biological replicates and graphed in order to examine the production of paramylon and corresponding MFI over the cultivation of the two strains. A two-way analysis of variance (ANOVA) was conducted for each of the parameters (paramylon/dry biomass, KO525-A and SSC-A) in order to assess whether there was significant variance in the paramylon content, fluorescence and granularity between the cultivation days and strains of *E. gracilis*. The significance level was set to alpha = 0.05.

2.8.6.2 Analysis of chlorophyll content

For investigation of chlorophyll fluorescence, the populations of bleached cells were gated and used as a relative baseline for measurement of chlorophyll MFI in the parameters PerCP and PC5.5 of unstained cells. MFI of PerCP and PC5.5 were normalised by cell concentration (cells/ml) as determined by FCM cell count per volume. Pearson's correlations were run between the chlorophyll content as determined by absorbance spectrophotometry and the FCM parameters PC5.5-A and PerCP-A to determine correlation coefficients. Scatter plots, with the linear regression lines, equations and R^2 values were plotted to determine goodness of fit. FCM result for MFI of PC5.5-A, PerCP-A and chlorophyll content by the absorbance assay were also averaged between biological replicates and plotted to examine the chlorophyll content and MFI over the cultivation of the two strains. A two-way ANOVA was conducted for each of the parameters (PC5.5-A, PerCP-5 and

chlorophyll content) to assess whether there was significant variance in chlorophyll and MFI between both the cultivation days and strains of *E. gracilis*. The significance level was set to alpha = 0.05.

2.8.6.3 Comparison of paramylon and chlorophyll during stationary phase of cell growth

Mean MFI for chlorophyll fluorescence (PC5.5-A and PerCP-A) were compared to mean side-scatter (SSC-A) MFI to investigate whether there was a relationship between chlorophyll and paramylon content as determined by flow cytometry. Side-scatter was used as the measure of paramylon as it had the strongest correlation with paramylon content as determined by the PSA assay. Analysis of both dry biomass and cell concentration flow cytometry revealed that cultures for both strains reached their stationary phase on day 4 (89 h) of cultivation. Pearson's correlations were calculated for the parameters from day 4 (89 h) to day 6 (137 h) to assess their relationship. Investigation was conducted during the stationary phase to avoid the effect of cell growth and division.

Chapter 3: Results

3.1 Auto-fluorescence spectra of *E. gracilis Z, Zm* and var. *saccharophila*

Auto-fluorescence spectra of three stains of *E. gracilis*; *Z, Zm* and var. *saccharophila* were grown in mixotrophic conditions and were examined to determine their suitability for fluorescence analysis and possible conflicts with fluorescent dyes. Selected excitations corresponded to wavelengths suitable for aniline blue and calcofluor white M2R, and to common lasers/filters available on fluorescence microscopy and FCM instruments. *E. gracilis Z* and var. *saccharophila* displayed similar spectral patterns (Figure 7).
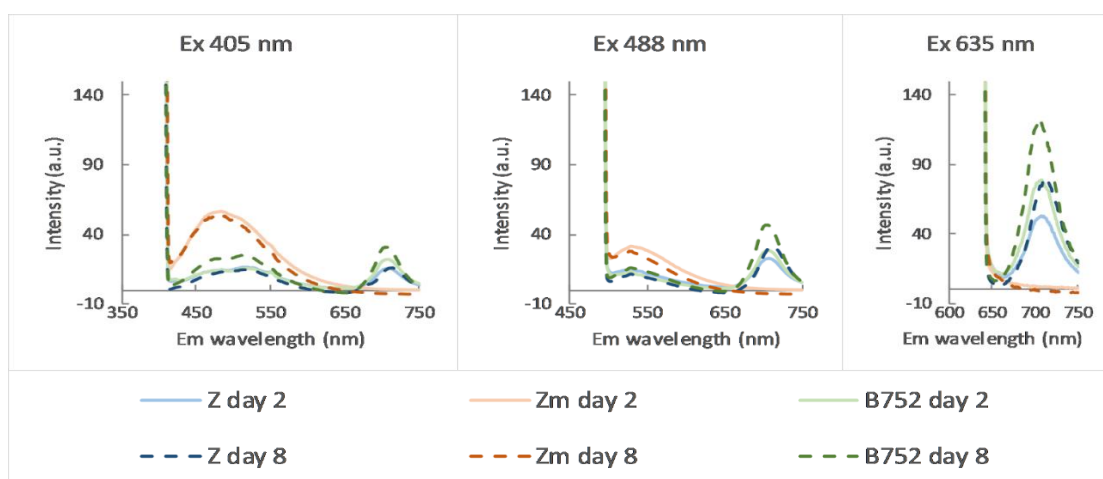
Figure 7. Mean auto-fluorescence spectra of *E. gracilis Z, Zm* and var. *saccharophila* (B) at excitation (Ex) wavelengths at 405 nm, 488 nm and 635 nm in biological triplicate using 'Cary Eclipse Fluorescence Spectrophotometer'. Spectra were taken from approximately 2×10^6 cells/ ml at day 2 (48 h) and day 8 (192 h) of cultivation with an excitation (Ex) slit width of 5 nm and emission (Em) slit width of 5 nm. Day 2 cells are represented by lighter solid lines and day 8 cells by darker dashed lines.

From Figure 7, it was evident that both *E. gracilis Z* and var. *saccharophila* displayed low and broad emission peaks from 450 nm – 550 nm when excited at 405 nm and a slight peak at 525 nm when exited at 488 nm. They also displayed relatively strong and sharp peaks at 700 nm with all three excitation lasers. The *Zm* strain produced a somewhat different spectrum. It displayed a higher blue fluorescence intensity 450 nm – 550 nm than the *Z* and var. *saccharophila* strains when excited at 405 nm and 488 nm, as well as a complete absence of fluorescence emission at 700 nm when excited with all three lasers. Aniline blue produces an aqua-green fluorescence emission (Em_{max} ~506 nm) when excited with violet light (405 nm) and calcofluor white M2R produces blue fluorescence emission (Em ~425 nm – 475 nm) when excited with near UV and violet light (350 nm – 405 nm). The criterion for using these dyes was that the *Euglena* strains should have low auto-fluorescence at 425 nm – 550 nm to avoid interfering with the fluorescent dye detection. This ruled out the *Zm* strain and therefore fluorescence microscopy and flow cytometry experiments were carried using only the *Z* and var. *saccharophila* strains.

3.2   Fluorescence microscopy of *E. gracilis Z* and var. *saccharophila*

Results of staining trials produced a method for fluorescent labelling of paramylon in *E. gracilis* using aniline blue. Calcofluor white M2R produced high levels of non-specific binding in both strains of *E. gracilis* and did not clearly label paramylon granules as displayed in Figure 8. It was therefore not used for further investigations.
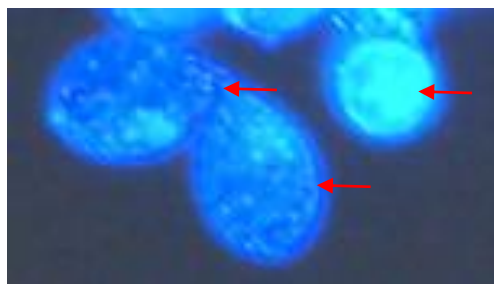
Figure 8. Fluorescence microscopy of *E. gracilis* var. *saccharophila* stained with calcofluor white M2R. Excitation 405 nm, Emission long pass filter 420 nm. Red arrows indicate cells where fluorescence is present throughout the cells. Individual granules are not visible.

To confirm successful staining and fluorescent labelling of paramylon in *E. gracilis* using aniline blue, stained and unstained cells from both day 3 (72 h) and day 6 (144 h) cultures were visualised using fluorescence microscopy. Microscopy was undertaken alongside quantification of paramylon per dry biomass to qualitatively compare fluorescent labelling to the concentration of paramylon within the cells being visualised.
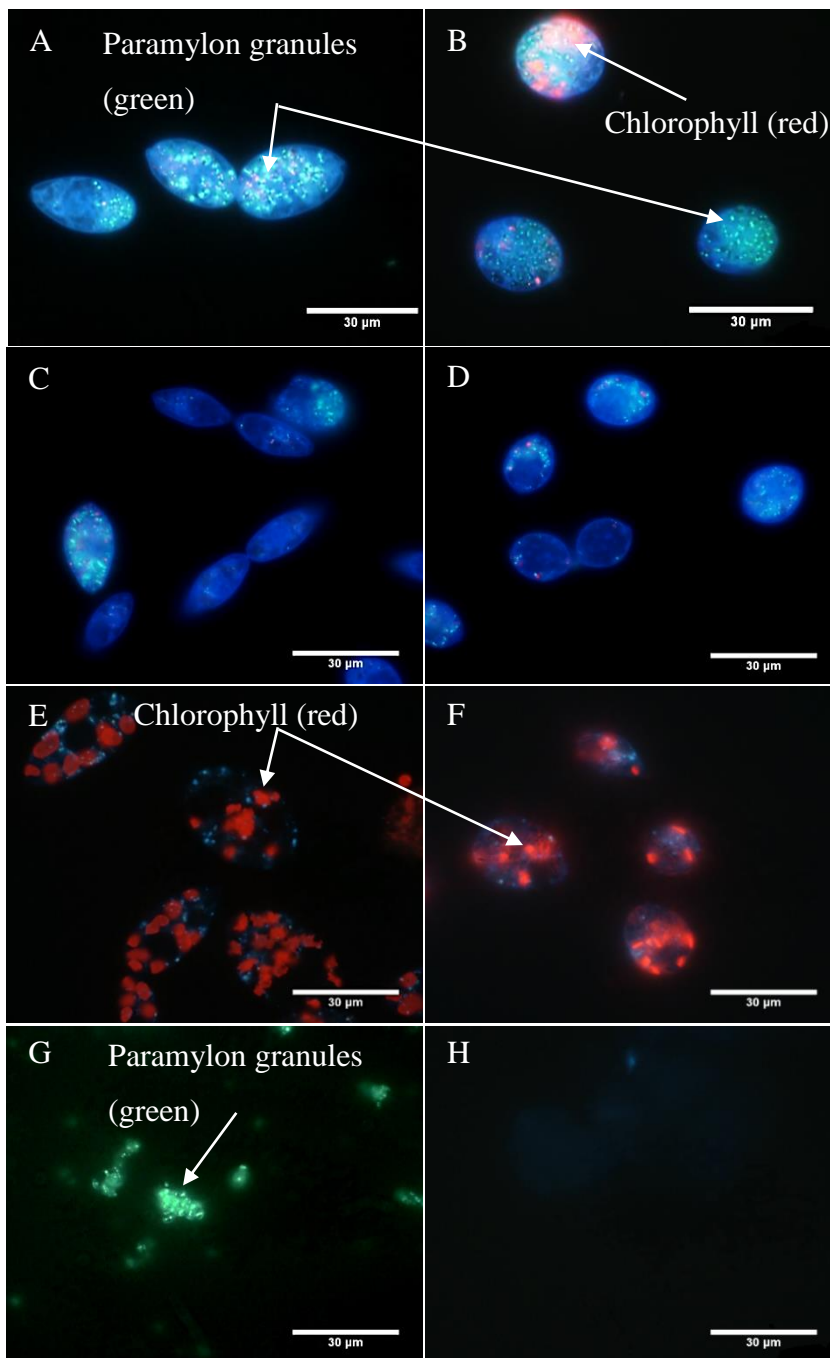
Figure 9. Fluorescence microscopy of *E. gracilis Z* (A, C, and E), *E. gracilis* var. *saccharophila* (B, D and F) and paramylon granules [β-1,3-glucan from Sigma Aldrich 89862-5-G] (G and H). Scale bar is 30 µm. Images taken with an 'Olympus BX 63 fluorescence microscope' and 'Olympus CellSens' software using a 330 – 385 nm excitation band pass, a DM 400 beam splitter and a 420 nm emission long pass filter. A and B: aniline blue stained day 3 (36 h) culture cells. C and D: aniline blue stained day 6 (144 h) culture. E and F: unstained/ control day 3 (36 h) culture cells. G: aniline blue stained paramylon granules. H: unstained control paramylon granules. Aniline blue labelled β-1,3-glucans are green, cell auto-fluorescence and dye blue, chlorophyll are red.

As shown in Figure 9, stained day 3 (72 h) cells of *E. gracilis Z* (2A) and *E. gracilis* var. *saccharophila* (2B) had many visible green fluorescent granules within the cells. However, the granules in var. *saccharophila* seemed dimmer and smaller than those of the *Z* strain. Stained day 6 (144 h) cells from both strains had fluorescent granules but to a lesser extent than the day 3 cells. Notably, all labelled cells produced strong blue fluorescence possibly due to either the dye or the staining procedure. While unstained cells (E and F) had some blue auto-fluorescence, it was to a much lower extent than in the stained samples. The presence of fluorescently labelled granules appeared to mirror the paramylon content in each strain and day as displayed in Figure 10. Here, both strains had increased levels of paramylon on day 3 compared to day 6, and the var. *saccharophila* strain had a

higher paramylon content than the *Z* strain. Additionally, both *Z* and var. *saccharophila* unstained cells did not appear to contain green fluorescent granules. However, they did contain some small blue auto-fluorescent particles and as well as relatively large red fluorescent organelles, which were most likely chloroplast. Finally, aniline blue stained β-1,3-glucan from *Euglena gracilis* [Sigma-Aldrich [89862-5g-F] (positive control) fluoresced green when excited with the near-UV/violet light, while unstained β-1,3-glucan did not. Together, these results indicate that the green fluorescence was due to the aniline blue and that paramylon *E. gracilis* cells was successfully stained.
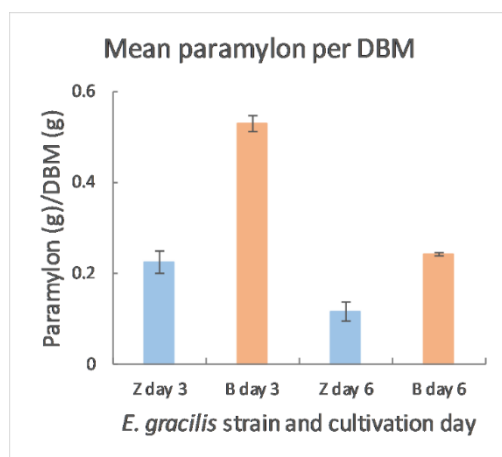
Figure 10. Mean paramylon content as a fraction of dry biomass (DBM) from biological triplicates of *E. gracilis Z* (Z) and var. *saccharophila* (B) after 3 days (36 h) and 6 days (144 h) of cultivation in *Euglena* medium under mixotrophic conditions. Error bars display standard deviation between the biological triplicates. Corresponding microscopy images in Figure 3: Z day 3 – A and E, B day 3 – B and F, Z day 6 – C, B day 6 – D.

3.3   Confocal microscopy of fluorescently labelled paramylon in *E. gracilis*

Confocal microscopy resulted in improved imaging of intracellular paramylon granules in *E. gracilis Z* and *E. gracilis* var. *saccharophila* as displayed in Figure 11. Figure 11 – 1A and 2A show fluorescence emitted from 500 – 560 nm from stained *E. gracilis Z* and var. *saccharophila* respectively when excited at 405 nm. In *E. gracilis Z* (1A) numerous fluorescent objects are clearly visible in the shape of 'dumbbells' or 'paired-dots'. This is too evident in var. *saccharophila* (2A), which, in addition, appeared to have fluorescent labelling of an outer oval region surrounding the bright centre. This indicated positive aniline blue staining for paramylon. Figure 11 – 1B and 2B display the same cells as imaged using the differential interference contrast (DIC) channel. This shows both cells packed with many oval-shaped granular structures (paramylon granules). When both the fluorescence and DIC channels were merged as displayed in 1C and 2C, the fluorescence 'dumbbells' appeared to overlap with the centre region of the granules. Notably. the top cell in 2A and 2C exhibited greater fluorescence than those by the lower cells. Figure 11 3A - 3C and 4A – 4C present the fluorescence, DIC and merged channels on unstained/negative control *E. gracilis Z* and var. *saccharophila* respectively. A small amount of background emission is visible, but the cells do not show the strong fluorescence present in the labelled cells, indicating that the fluorescence in stained cells was due to the labelled paramylon.
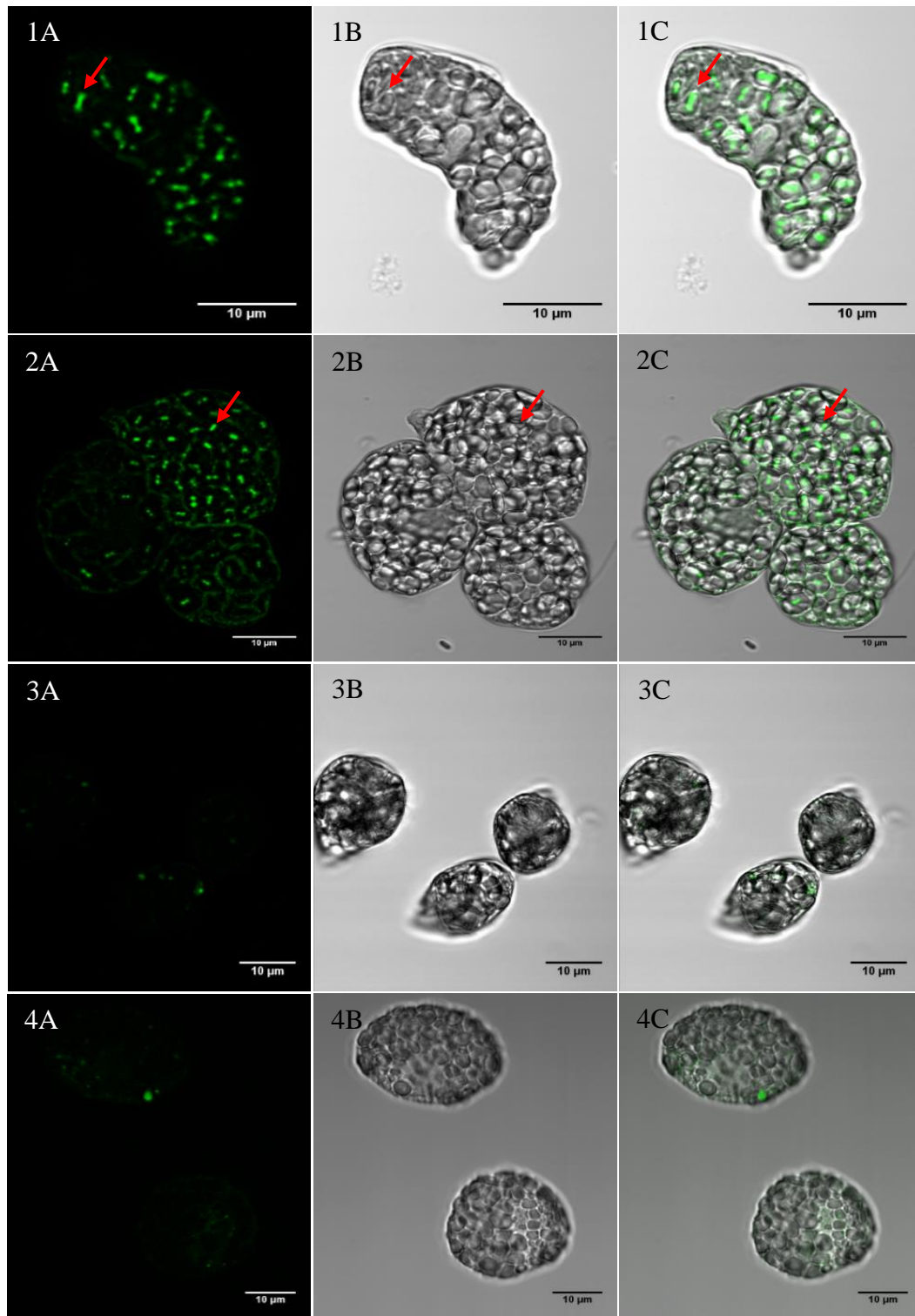
Figure 11. Confocal microscopy of fluorescently labelled and unlabelled *E. gracilis Z* and E. *gracilis* var. *saccharophila* taken with an Olympus fluorview FV1000 IX81 inverted confocal microscopy. Paramylon granules within cells were labelled with aniline blue (methyl blue - Sigma-Aldrich [M6900]) and detected fluorescence is displayed in green. 1: labelled *E. gracilis Z*. 2: labelled *E. gracilis* var. *saccharophila*. 3: unlabelled control *E. gracilis Z*. 4: unlabelled control *E. gracilis* var. *saccharophila*. A: fluorescence image Ex 405nm, Em 530/30 nm. B: DIC channel. C: merged fluorescence and DIC channels. Red arrows indicate location of a paramylon granule in each strain.

3.4 Flow cytometry analysis of *E. gracilis*

3.4.1 Correlation of paramylon content: flow cytometry vs. phenol-sulphuric acid hydrolysis assay and dry biomass

In order to validate the use of flow cytometry for assessment of paramylon content, Pearson's correlation was used to examine the relationship between FCM analysis and paramylon content per dry biomass via the PSA assay. During FCM, labelled paramylon fluorescence was measured via the arbitrary unit of medium fluorescence intensity (MFI) using a 525/40 nm band pass filter with 405 nm violet light excitation per area of signal intensity (KO525-A). Similarly, relative cell granularity was measured using side/right angle light scatter (SSC-A) and cell size via forward light scatter (FSC), as it was expected that both these parameters would be influenced by the number and size of the paramylon granules present in the cells. Thus, paramylon content was correlated with MFI of stained and unstained control cells for the FCM parameters KO525-A, SSC-A and FSC-A.

Results displayed in Figure 12, Table 8 and Table 9 show that correlations of FCM parameters with paramylon content were highly significant. A fairly strong relationship was shown with the FCM parameter for aniline blue fluorescence (KO525) in *E. gracilis Z* as displayed by the linear regression line in the scatter plot of Figure 12A. Pearson's correlation gave a coefficient (r) of 0.9082 and coefficient of determination (R^2) of 0.8247, thus a large percentage of the variation in paramylon content could be explained by aniline blue fluorescence. This relationship was weaker for *E. gracilis* var. *saccharophila* (Figure 12A and Table 9) with r and R^2 values of 0.847 and 0.7175 respectively. The strongest correlation between paramylon content and flow cytometry MFI as shown in Table 8 and Table 9 was with side scatter of unstained control cells. The weakest correlations were between paramylon content and forward scatter of the stained cells (equivalent to cell size).

In general, *E. gracilis Z* had higher correlation coefficients than *E. gracilis* var. *saccharophila* and unstained control cells had stronger correlations than the stained cells between the paramylon content and both FSC and SSC. Therefore, quantified paramylon content was more closely related to MFI in *Z* strain (i.e. FCM was more accurate for *E. gracilis Z*) and while labelled fluorescence was positively associated paramylon content, SSC appeared to be the stronger measure.
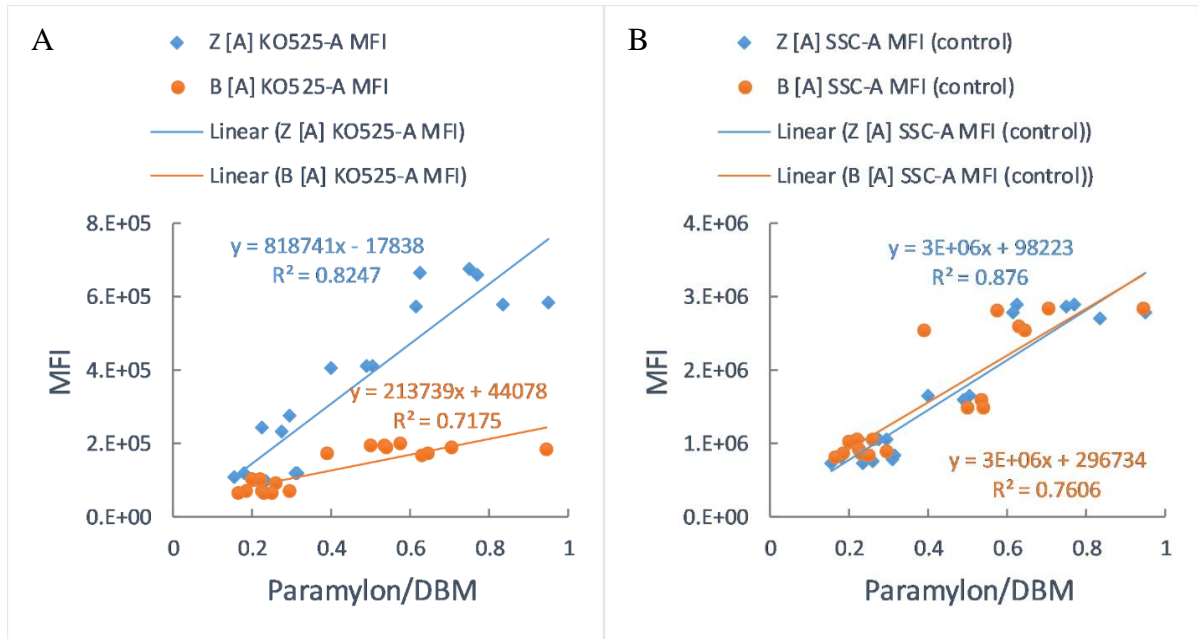
Figure 12. Scatter plots and regression lines for paramylon content of FCM median fluorescence intensity (MFI). The positive correlation of A: aniline blue fluorescence (K0525-A) and B: SSC granularity (SSC-A) MFI, with paramylon content per dry biomass (DBM) as determined by PSA assay and absorbance in *E. gracilis Z* and var. *saccharophila* (B).

Table 8. Correlation of paramylon per dry biomass with flow cytometry median fluorescence intensities for *E. gracilis Z*. Key: KO525-A = aniline blue labelled fluorescence, SSC-A = side scatter/granularity, FSC-A = forward scatter/size, stained = cells that were stained with aniline blue and unstained = control cells that were not stained with aniline blue.

Pearson r	*Z* paramylon vs. KO525-A (stained)	*Z* paramylon vs. SSC-A (stained)	*Z* paramylon vs. SSC-A (unstained)	*Z* paramylon vs. FSC-A (stained)	*Z* paramylon vs. FSC-A (unstained)
r	0.9082	0.9284	0.9359	0.8772	0.9306
95% confidence interval	0.7661 to 0.9656	0.8147 to 0.9734	0.8331 to 0.9762	0.6948 to 0.9535	0.8201 to 0.9742
R squared	0.8247	0.862	0.876	0.7694	0.8661
P value (two-tailed)	<0.0001	<0.0001	<0.0001	<0.0001	<0.0001

Table 9. Correlation of paramylon per dry biomass with flow cytometry median fluorescence intensities for *E. gracilis* var. *saccharophila* (B). Key: KO525-A = aniline blue labelled fluorescence, SSC-A = side scatter/granularity, FSC-A = forward scatter/size, stained = cells that were stained with aniline blue and unstained = control cells that were not stained with aniline blue.

Pearson r	B paramylon vs. KO525-A (stained)	B paramylon vs. SSC-A (stained)	B paramylon vs. SSC-A (unstained)	B paramylon vs. FSC-A (stained)	B paramylon vs. FSC-A (unstained)
r	0.8470	0.8686	0.8721	0.7394	0.8413
95% confidence interval	0.6288 to 0.9416	0.6757 to 0.9501	0.6836 to 0.9515	0.4163 to 0.8967	0.6166 to 0.9393
R squared	0.7175	0.7544	0.7606	0.5468	0.7078
P value (two-tailed)	<0.0001	<0.0001	<0.0001	0.0005	<0.0001

3.4.2   Analysis of paramylon content by flow cytometry and acid hydrolysis (PSA)

Flow cytometry alongside the PSA assay were used to monitor the paramylon per dry biomass across a 6-day cultivation period for *E. gracilis Z* and var. *saccharophila* in mixotrophic conditions. Results are displayed in Figure 13, which show that both paramylon (6A), aniline blue fluorescence (6B) and side scatter (6C), peaked early on days 1 (17 h) and 2 (41 h), and then steadily declined over the cultivation period. While paramylon content and side scatter MFI looked similar for both strains, MFI of the fluorescently labelled (KO525) var. *saccharophila* strain cells appeared to be much weaker than that of the *Z* strain cells. This suggests inefficient staining or inefficient binding of the fluorophore in the var. *saccharophila* strain cells. Paramylon content shown is per dry biomass and MFI is per event/cell. Side scatter can be used for both labelled and unlabelled cells, but is only shown here for unstained cells.
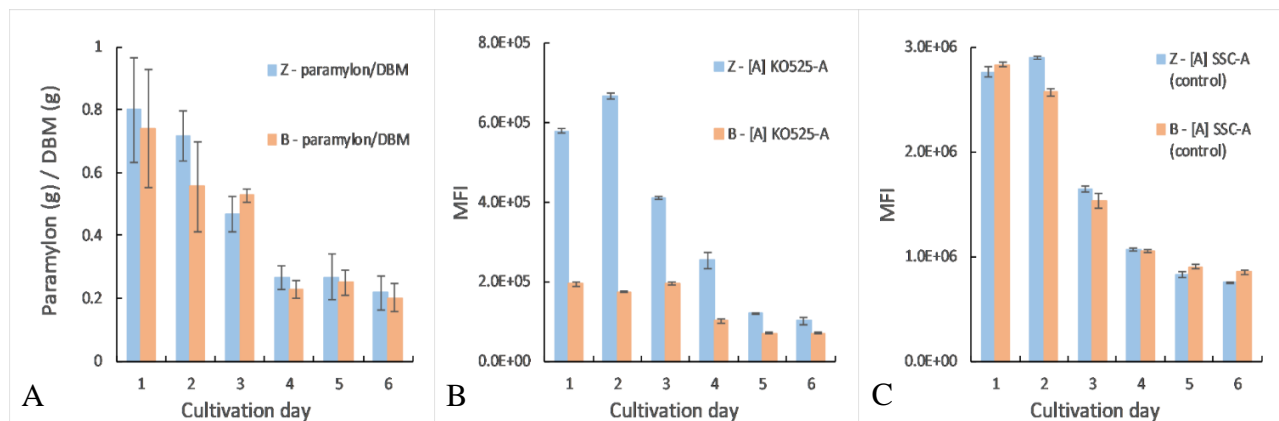
Figure 13. Analysis of mean paramylon content in *E. gracilis* Z (Z/blue) and *E. gracilis* var. *saccharophila* (B/orange) across 6-day cultivation in *Euglena* medium under mixotrophic conditions. A: paramylon content per dry biomass (DBM) determined by PSA assay. B: FCM MFI (arbitrary units) for KO525-A BP (525/40 nm) fluorescence of aniline blue labelled cells. C: FCM MFI (arbitrary units) for SSC-A scatter (granularity) of control/unlabelled cells. Black bars represent standard deviation of the biological triplicates.

There was an obvious variation across cultivation times, but it was not clear from direct observation of paramylon content and MFI if there was a difference between the strains. Therefore, statistical analysis was undertaken to assess whether there was a significant difference between the two strains. In addition, this allowed a comparison between detection methods, to see if the PSA assay or FCM could detect a difference that the other could not. A two-way analysis of variance (ANOVA) was used to assess whether there was statistically significant variance in paramylon content, fluorescence (KO525) and granularity (SSC) between *E. gracilis* strains and across the cultivation days.

In the 2-way ANOVA of paramylon/dry biomass by biochemical determination (PSA), the cultivation day had a major effect on the variation of paramylon content (85.9% of total variation). However, type of strain had no significant impact and there was not significant interaction between strain type and cultivation time (see Table 10). In the analysis of KO525 MFI, cultivation day (47.74%), strain of *E. gracilis* (33.02%) and the interaction between the two variables (19.13%) all had a significant effect on the variation in MFI and thus paramylon content (see Table 10). Lastly, the 2-way ANOVA for SSC of unstained cells suggested that cultivation day had a highly significant and major effect on MFI as it was responsible for 99.08% of total variation. Yet, despite only accounting for a miniscule percentage of total variation, strain type (0.04113%) had a highly significant effect on MFI. Additionally, there also seemed to be an interaction between the strain and cultivation time. Together the results confirm that there were differences in paramylon content of *E. gracilis Z* and *E. gracilis* var. *saccharophila* across the cultivation times/days and indicate that there may have been a small difference in paramylon content between the strains. The results also suggest that FCM may have superior detection capabilities and sensitivity than the biochemical PSA quantification method.

Table 10. Two-way ANOVA (ordinary) for analysis of variance in measured paramylon content between strains of *E. gracilis* (Z and var. *saccharophila*) and cultivation days (days 1 – 6). Separate analysis was undertaken for the three measures of paramylon: paramylon per dry biomass (top), KO525-A median fluorescence intensity (middle), SSC-A median fluorescence intensity (bottom). Family-wise significance level was set to 0.05 (95% confidence interval).

Parameter	Source of variation	% of total variation	F (DFn, DFd)	P value
Paramylon/dry biomass (PSA)	Interaction	2.029	F (5, 24) = 0.86	0.5245
	Cultivation day	85.9	F (5, 24) = 36.24	<0.0001
	Strain	0.6931	F (1, 24) = 1.46	0.2384
KO525-A (FCM)	Interaction	19.13	F (5, 24) = 834.1	<0.0001
	Cultivation day	47.74	F (5, 24) = 2082	<0.0001
	Strain	33.02	F (1, 24) = 7200	<0.0001
SSC-A (FCM)	Interaction	0.7845	F (5, 24) = 39.38	<0.0001
	Cultivation day	99.08	F (5, 24) = 4973	<0.0001
	Strain	0.04113	F (1, 24) = 10.32	<0.0037

3.4.3   Correlation of chlorophyll content: flow cytometry and absorbance spectrophotometry

Flow cytometric analysis using blue (488 nm - PerCP-A) and yellow (561 nm – PC5.5-A) laser excitation with far red fluorescence emission detection (690/50 nm) was also explored as a tool for montitoring the metabolic state of *E. gracilis* throughout their cultivation. In order to validate the detection of chlorophyll by FCM, median chlorophyll fluorescence intentsity was correlated to chlorophyll content as determined by absorbance spectrophotometry as described by Jeffrey, et al. [137]. As shown by the regression line in the scatter plot for *E. gracilis Z* (Figure 14A) and correlation results in Table 11. There was a strong positive relationship for both chlorophyll content in mg/ml and PC5.5-A MFI*cells/ml ($r = 0.9677$, $R^2 = 0.9364$, $p < 0.0001$) and chlorophyll content and PerCP-A MFI*cells/ ($r = 0.9766$, $R^2 = 0.9537$, $p < 0.0001$). The significance level was set at alpha = 0.05. Figure 14B displays the scatter plot a for total chlorophyll content (mg/ml) with the FCM paramaters for *E. gracilis* var. *saccharophila*. Results of the correlation for the var. *saccharophila* strain are also given in Table 11. There was a significant positive correlation between both chlorophyll content (mg/ml) and PC5.5-A*cells/ml ($r = 0.9804$, $R^2 = 0.9612$ $p <.0001$) and between chlorophyll content and PerCP-A*cells/ml ($r = 0.9822$, $R^2 = 0.9646$, $p < .0001$) with a signifcance level of alpha = 0.05. Results indicated that both FCM parameters strongly correlated with the total chlorophyll content in both *E. gracilis* strains, validating the use of FCM for relative quantification of chlorophyll.

Table 11. Correlation of total chlorophyll content as determined by absorbance spectrophotometry in mg/ml against chlorophyll median fluorescence intensity*cells/ml in both *E. gracilis Z* (Z) and *E. gracilis* var. *saccharophila* (B). Key PC5.5-A = chlorophyll fluorescence by signal intensity area with yellow excitation laser (Ex 561nm, Em 690/50 nm BP) and PerCP-A = chlorophyll fluorescence by signal intensity area with blue excitation laser (Ex 488 nm, Em 690/50 nm BP).

Pearson r	Z chlorophyll (mg/ml) vs. PC5.5-A* cells/ml	Z chlorophyll (mg/ml) vs. PerCP-A* cells/ml	B chlorophyll (mg/ml) vs. PC5.5-A* cells/ml	B: chlorophyll (mg/ml) vs. PerCP-A* cells/ml
r	0.9677	0.9766	0.9804	0.9822
95% confidence interval	0.9135 to 0.9881	0.9368 to 0.9914	0.947 to 0.9928	0.9517 to 0.9935
R squared	0.9364	0.9537	0.9612	0.9646
P value (two-tailed)	<0.0001	<0.0001	<0.0001	<0.0001
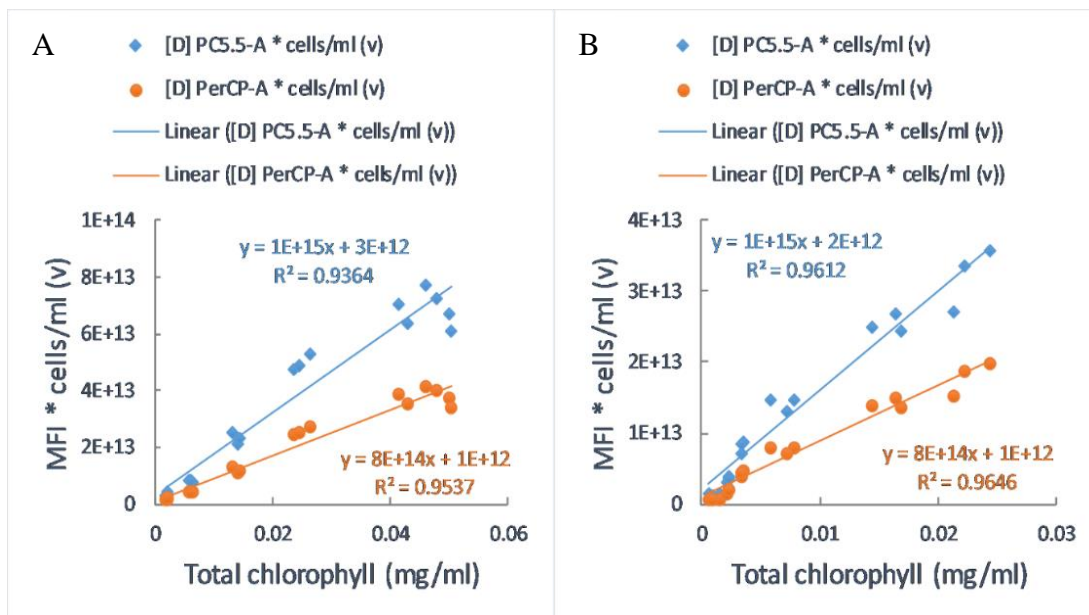
Figure 14. Scatter plots with linear regression lines, equations and R^2 value for total chlorophyll content (determined by absorption readings) against FCM fluorescence (MFI*cells/ml). The positive correlations of total chlorophyll content with the FCM parameters PC5.5-A (Ex 561nm, Em 690/50 nm BP) and PerCP-A (Ex 488 nm, Em 690/50 nm BP) are represented in 'blue' and 'orange' respectively for *E. gracilis Z* (A – left) and *E. gracilis* var. *saccharophila* (B- right).

3.4.4 Analysis of chlorophyll content via absorbance and fluorescence intensity

Absobance spectrophotometry, and FCM were used to monitor the chlorophyll content in *E. gracilis* Z and *E. gracilis* var. *saccharophila*. Samples were taken from cultures and at the same time as those analysed for paramylon content in section 3.4.2. Results in Figure 15 showed an increase in chlorophyll content over the cultivation period as determined by absorbance spectrophotometry (9A) and by the FCM parameters PC5.5-A (7B) and PerCP-A (7C). In all three measures the Z strain (Z – shown in blue) had approximately more than double the chlorphyll content than var. *saccharophila* (B – shown in orange) on each day of cultivation.
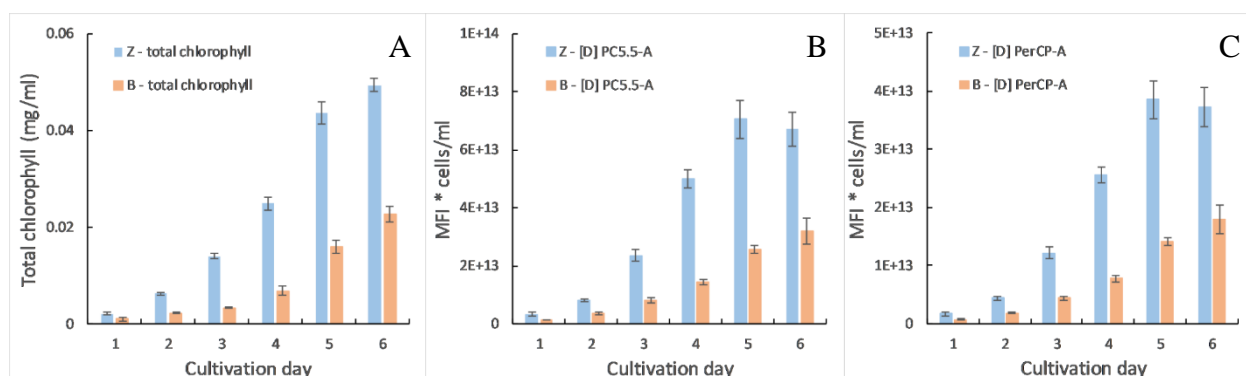
Figure 15. Analysis of mean chlorophyll content in E. *gracilis* Z (Z – blue) and *E. gracilis* var. *saccharophila* (B – orange) across 6-day cultivation in *Euglena* medium under mixotrophic conditions. Black bars indicated standard deviation of the mean from biological triplicates. A: total chlorophyll content (a + b) as determined by absorbance spectrophotometry [137] in mg/ml. B: FCM PC5.5-A MFI * cells/ml (Ex 561nm, Em 690/50 nm BP). C: FCM PerCP-A MFI * cells/ml (Ex 488 nm, Em 690/50 nm BP).

While the the variation in chlorophyll content and MFI was more immediatelly apparent for chlorophyll analysis. A two-way ANOVA was undertaken in to confirm the variation across the cultivation times and between *E. gracilis* Z and *E. gracilis* var. *saccharophila*. Results are displayed in Table 12, all results were highly significant (p <.0001). For the analysis of total chlorophyll content by absorbance spectrophotometry (mg/ml), the cultivation time/day had the largest impact (66.84% of variation), followed by the strain type (22.03%) and the interaction between cultivation day and strain (10.79%). Similar result were attained for the FCM chlorophyll fluorescence paramters PC5.5-A (Ex 561 nm, Em 690/50 nm) and PerCP-A (Ex 488 nm, Em 690/50 nm) with cultivation time having the largest impact on variation in MFI, followd by the effect of the strain of *E. gracilis* and interaction between the two variable having the least impact (see Table 12). In summary, the analysis of chlorophyll content via absorbance spectrophotemetry and FCM produced similar results. The 2-

way ANOVA indicated that the chlorophyll content of *E. gracilis Z* was siginficantly greater than that of var. *saccharophila*; and that the chlorophyll content significantly increased over the period of cultivation. These results successfully showcase that FCM can be used of chlrophyll analysis in *E. gracilis*.

Table 12. Two-way ANOVA (ordinary) for analysis of variance in chlorophyll content between strains of *E. gracilis* (Z and var. *saccharophila*) and cultivation days (days 1 – 6). Separate analysis was undertaken for the three measures of chlorophyll content: chlorophyll content as determined by absorbance spectroscopy (top), FCM PC5.5-A MFI*cells/ml (middle), and FCM PerCP-A MFI*cells/ml (bottom). Family-wise significance level was set to 0.05 (95% confidence interval).

Parameter tested	Source of variation	% of total variation	F (DFn, DFd)	P value
Chlorophyll (mg/ml)	Interaction	10.79	$F_{(5, 24)} = 147.2$	<0.0001
	Cultivation day	66.84	$F_{(5, 24)} = 912.3$	<0.0001
	Strain	22.03	$F_{(1, 24)} = 1503$	<0.0001
FCM PC5.5-A *cells/ml	Interaction	12.01	$F_{(5, 24)} = 51.03$	<0.0001
	Cultivation day	63.49	$F_{(5, 24)} = 269.8$	<0.0001
	Strain	23.37	$F_{(1, 24)} = 496.5$	<0.0001
FCM PerCP-A *cells/ml	Interaction	11.66	$F_{(5, 24)} = 52.34$	<0.0001
	Cultivation day	65.23	$F_{(5, 24)} = 292.9$	<0.0001
	Strain	22.04	$F_{(1, 24)} = 494.9$	<0.0001

3.4.5 Comparison of paramylon and chlorophyll content using flow cytometry

Lastly, FCM was used to examine the relationship between paramylon and chlorophyll content in *E. gracilis* and whether they could be used in conjunction to monitor the metabolic state of the cells. Side scatter (SSC-A) MFI of the unstained *E. gracilis* cells was used as the measure of paramylon was used due to its strong correlation with quantified paramylon content via the PSA assay. This was compared to the MFI of the two parameters used to measure chlorophyll content: yellow laser – 650/90 nm red emission (PC5.5) and blue laser – 690/50 nm red emission (PerCP). From Figure 16A, it can be seen that while MFI for side scatter steadily declined over the course of the cultivation, MFI for chlorophyll fluorescence dropped from between days 1-3 and then increased between days 3-6. Notably, this increase coincided with the *E. gracilis* cultures reaching the stationary phase of growth as shown in Figure 16B. A Pearson's correlation from days 4-6 between SSC-A and PC5.5-A (r = -0.99.03, p < .0001) and PerCP (r = -0.98.40, p < .0001) gave strong negative correlations for *E.*

gracilis Z. Strong negative correlations were also observed for *E. gracilis* var. *saccharophila* (SSC-A/PC5.5: r = -0.9737, p < .0001. SSC-A/PerCP-A: r = -0.9733). Linear regression lines and coefficient of determination (R^2) were plotted to assess the goodness of fit in Figures 16C and 16C for *E. gracilis Z* and var. *saccharophila* respectively. All slopes were significantly non-zero (p < .0001, for alpha = 0.05). Together this suggests that there was a relationship between paramylon and chlorophyll in the cells, where by cellular utilisation of paramylon coincided with increasing development of chlorophyll and thus reliance of the cells on photosynthesis.
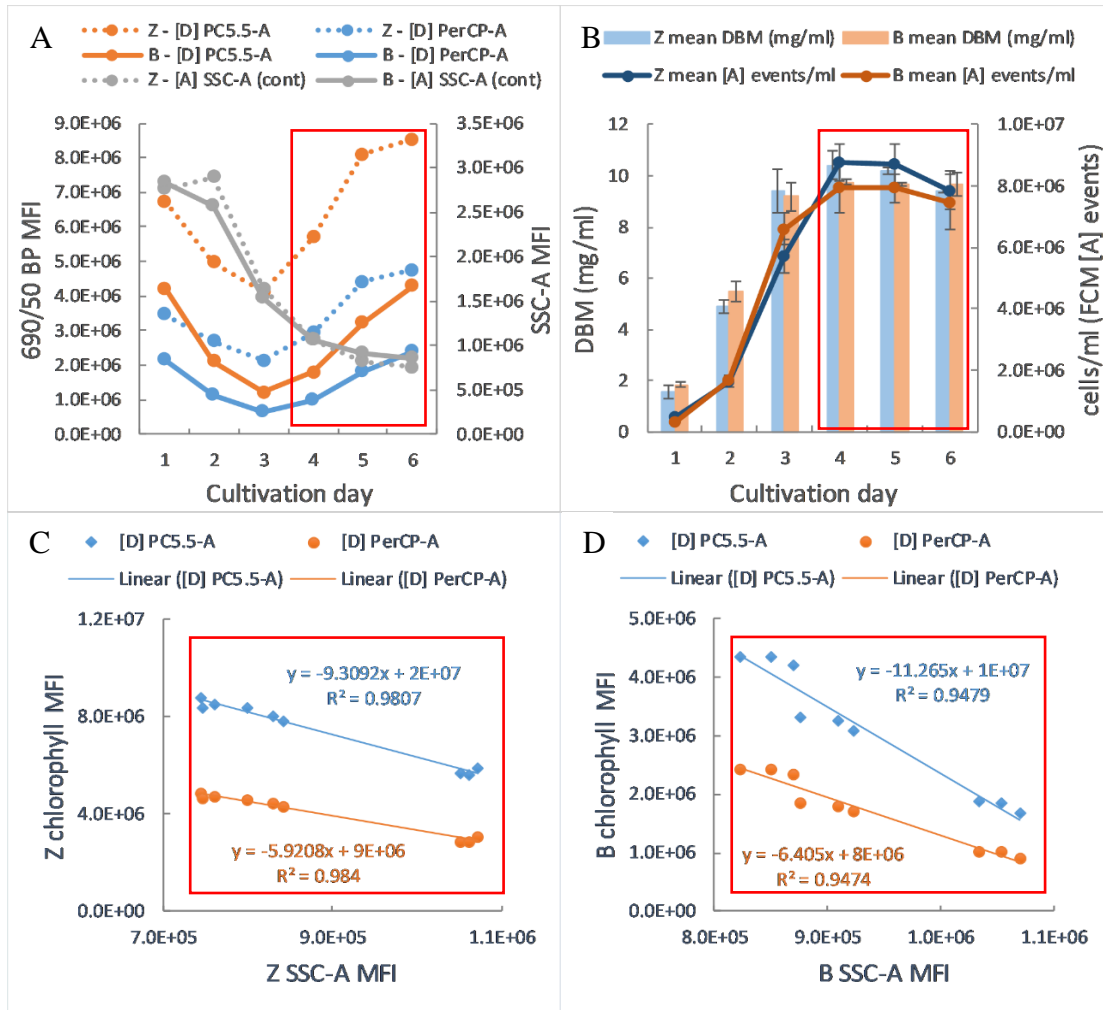
Figure 16. Comparison of FCM measurement of paramylon content in unstained cells by side-scatter (SSC-A) and chlorophyll content by red fluorescence (PC5.5-A and PerCP-A). Red box indicates data from day 4 – 6 culture samples. A: FCM PC5.5-A and PerCP-A (chlorophyll - Em690/50 nm) MFI (left axis) compared to FCM SSC-A (control cells) MFI (right axis) over cultivation. B: mean growth of *E. gracilis Z* and *E. gracilis* var. *saccharophila* across 6-day cultivation period measured by dry biomass (DBM) in mg/ml (columns) and FCM cell count (lines). Linear regression of SSC-A MFI against PC5.5-A and PerCP-A MFI for *E. gracilis Z*. Linear regression of SSC-A MFI against PC5.5-A and PerCP-A MFI for *E. gracilis* var. *saccharophila* (B).

3.6   Results summery

In summary, auto-fluorescence of the strains was first assessed to determine their suitability for fluorescence analysis and possible conflicts that could arise with fluorescent dyes. A staining method was successfully developed for fluorescence detection of paramylon with the dye aniline blue for two of the strains; *E. gracilis Z* and *E. gracilis* var. *saccharophila*. Specifically, the binding of the dye's fluorophore to paramylon granules was assessed using fluorescence and confocal microscopy. Lastly, Z and var. *saccharophila* stains were cultivated over a 6-day period, showcasing the ability of flow cytometry (FCM) to detect paramylon content and monitor chlorophyll development. Median fluorescence intensity (MFI) from FCM were validated against quantification of paramylon per dry biomass using the phenol-sulphuric acid hydrolysis assay and chlorophyll content via absorbance spectrophotometry. The relative effects of cultivation time and strain type on paramylon and chlorophyll content were assessed and the relationship between paramylon and chlorophyll was examined.

Chapter 4: Discussion

E. gracilis is a species of microalgal protist with great potential as nutritious food source and industrial producer of valuable compounds. It can survive in a wide range of cultivation conditions, has a high photosynthetic productivity and accumulates the valuable β-1,3-glucan paramylon as a reserve polysaccharide. Investigations of paramylon in *E. gracilis* have primarily been focused on optimising cultivation conditions and have utilised gravimetric, biochemical and absorbance based methods of quantification. For the continued improvement of paramylon production in *E. gracilis*, high-throughput methods for optimising cultivation and screening viable strains would be highly advantageous. In this work two strains/variants of *E. gracilis* were assessed for their production of paramylon, as well as their growth and development of chlorophyll. The goal of the work was to explore the strains using fluorescence and light-scatter based high-throughput methods, with a view of developing a platform upon which future screening and potential sorting of desirable strains, mutants and/or recombinants, and optimisation of paramylon production may be achieved.

4.1   Fluorescence spectrophotometry of auto-fluorescence in *E. gracilis*

Microalgae, including *E. gracilis* can emit high levels of auto-fluorescence, especially from photosynthetic pigments. This can be utilized for measurements of algal pigments, but become noise during microscopy and FCM, and interfere with detection of fluorescent dyes and probes [72, 111]. Therefore, the auto-fluorescence spectrum of the initial three strains of *E. gracilis* (Z, Zm and var. *saccharophila*) were examined to determine their suitability for fluorescence analysis with the dyes

aniline blue and calcofluor white M2R. When excited at 405 nm and 488 nm, all three strains displayed some level of blue-green auto-fluorescence (400 – 550 nm), with the highest being exhibited by the *Zm* strain (Figure 7). This blue-green fluorescence has been noted previously and is suggested to result from photoreceptor pigments, most likely a rhodopsin-like photoreceptor protein *Erh* [150] and/or pterin and flavin molecules located in the paraflagellar bodies and vesicles within the alga [151, 152]. Schmidt, et al. [151] also noted that blue fluorescence was heightened in chlorophyll free mutants, which lacking chloroplasts had reduced noise from chlorophyll fluorescence and thus enhanced blue fluorescence detection. This may help explain why the *Zm* strain seemed to exhibit a higher blue-light emission intensity. Thus, the *Zm* strain was excluded from further experiments as its auto-fluorescence could have interfered with the emission from the fluorescent dyes.

In addition to the blue light auto-fluorescence, both *E. gracilis* Z and var. *saccharophila* produced red fluorescence peaks (at approximately 700 nm) when excited at 405 nm, 488 nm and 635 nm, while the bleached *Zm* strain did not. This is consistent with fluorescence produced by chlorophyll which *E. gracilis* are known to contain [153, 154]. Thus, both strains could be utilised for analysis of chlorophyll content by FCM, enabling monitoring of metabolic state and examination of the relationship between paramylon and chlorophyll content in the cells.

4.2   Microscopy and fluorescence labelling of intracellular paramylon

Fluorescence and confocal microscopy were used to assess the fluorescent labelling of paramylon granules in *E. gracilis* Z and *E. gracilis* var. *saccharophila*. This was carried out to develop a protocol that could be used to label and detect paramylon content using flow cytometry. Fluorescence microscopy (Olympus Bx63) was first implemented for examining various labelling conditions for the dyes aniline blue and calcofluor white M2R in order to develop a working fluorescent staining protocol (see section 2.5). Staining with aniline blue was successful. Calcofluor white M2R produced high levels of non-specific binding which interfered with the ability to view any labelled granules.

In order to visualise successful fluorescent labelling, *E. gracilis* Z and var. *saccharophila* were cultivated under mixotrophic conditions in *Euglena* medium. Cells were harvested at day 3 (72 h) and day 6 (144 h), labelled and visualised, alongside quantification of paramylon by PSA and dry biomass. It should be noted that while the PSA assay is not specific for paramylon, it has previously been used for the quantification of paramylon in *E. gracilis* as the only carbohydrate present in substantial quantity that is resistant to acid hydrolysis or solubilisation [59, 74]. Fluorescent imaging

demonstrated that both strains were successfully labelled, with the younger cultures appearing to have greater fluorescent labelling and thus more paramylon than the older cultures. This trend corresponded with the PSA and gravimetric quantification of the paramylon content. From the images it was difficult to compare labelled paramylon content between the two strains despite the biochemical quantification showing what appeared to be major differences in paramylon content. The commercially supplied stained granules displayed green fluorescence, and the unstained cells and granules did not display green fluorescence. Examination of the auto-fluorescence spectra of *E. gracilis Z* and var. *saccharophila* revealed relatively large red chloroplasts and smaller blue objects were apparent in the unstained negative control cells (Figure 9E and 9F). Also, blue fluorescence appeared throughout the stained cells which did not appear in the controls (which only had small localised blue objects). Thus, despite decolourising the aniline blue dye, the cells retained significant blue staining. This suggests that the major non-fluorochrome portion of the dye was bound to some other component within the cells. While the dye portion of aniline blue has been used to stain collagen [155], *E. gracilis* are not known to contain collagen [30]. *Euglena* cells are enclosed within a semi-ridged, predominantly protein pellicle which supports the cell membrane [34, 136, 156]. This could be a possible candidate for the binding of the dye and thus presence of the blue fluorescence and could be tested by isolating and staining the pellicle. To reduce binding and thus fluorescence from the dye itself, labelling of *E. gracilis* could be carried using purified aniline blue fluorophore 'Sirofluor' [128, 157] or a (1→3,1→4)-β-glucan-specific monoclonal antibody [158]. While not employed in this work, either of these could be used for further improvement and optimisation of fluorescent labelling of paramylon in *E. gracilis*.

To confirm fluorescent labelling, confocal microscopy utilising both fluorescence (530/30 nm band pass) and differential interference contrast (DIC), was used to image aniline blue labelled *E. gracilis* cells. This enabled enhanced detection of the fluorescence with reduced background and auto-fluorescence by employing a narrower bandwidth for detection of emitted light. In addition to improved fluorescence imaging, confocal microscopy enabled the implementation of DIC imaging, which enhanced the contrast of the normally transparent granules. Merging of the fluorescence and DIC images allowed the fluorescence to be overlayed on to the granules. In the imaging of the var. *saccharophila* strain (Figure 11 – *2*) the outer surface of the granules also appeared to emit fluorescence; however, only one of these cells appeared to have strong binding and fluorescence. This could be a result of inefficient uptake or binding of aniline blue in *E. gracilis* var. *saccharophila*. During imaging, only thin image stacks could be taken due to rapid bleaching of the fluorophore. Therefore, the reduced fluorescence emitted from the lower two cells (Figure 11 – 2) may have been

due to bleaching of the fluorophore or the cells not being within the correct focal plane. Nevertheless, the confocal imaging undertaken here confirmed the binding of the aniline blue fluorophore to the granules and presents the first fluorescent labelling of intracellular paramylon in *E. gracilis*.

In addition, the binding and fluorescence pattern of the aniline blue fluorophore could be explained by the structure of the paramylon granules themselves. For example, in both strains that were labelled, the fluorescence was emitted predominantly from the inner/centre region of the granules and had elongated 'dumbbell' shapes or existed as pairs of close dots as seen in Figure 11. Previous investigations of the structure of euglenoid paramylon have found that the granules are highly crystalline and enclosed in a membrane. The granules are composed of rectangular and triangular shaped segments composed of concentric layers of micro fibril bundles which meet in a central region [159-161]. An X-ray and dissolution study of the granules by Kiss, et al. [160] also noted that this central region was differently organised than the other parts of the granules and had tighter packing of the micro fibrils. The shape of this central hilum described by Kiss, et al. [159] appear to match the fluorescence emitted from paramylon granules. Furthermore, it has also been observed that β-1,3-glucans have a triple-helical conformation that partially opens upon exposure to alkaline pH with NaOH and results in a higher biological activity [162]. As such, it may also be possible that the addition of NaOH in the staining procedure aided in enhancing fluorescence, however it is uncertain as to why the granule hilum would have a more biologically active conformation than the outer segment regions. Nevertheless, labelling may have been improved by the addition of NaOH and the location of the fluorescence may be explained by the fluorophore binding predominantly to the granule hilum due to the organisation and packing of the paramylon micro fibrils.

4.3 Comparison of flow cytometry and biochemical assessment for determination of paramylon in *E. gracilis*

The relationship between median fluorescence intensity of the examined flow cytometry (FCM) parameters and the quantified paramylon via the PSA assay was assessed using a correlation analysis. This examination compared FCM and PSA results from *E. gracilis Z* and *E. gracilis* var. *saccharophila* over a 6-day cultivation period. Significance level of the analysis was set to alpha = 0.05. Results gave strong correlation (r) and goodness of fit (R^2) between the quantified paramylon content (PSA/dry biomass) and flow cytometry fluorescence (KO525-A), side scatter (SSC-A) and forward scatter (FSC-A). Stronger results were attained for the *Z* strain as opposed to var. *saccharophila.* For both strains of *E. gracilis,* the strongest correlation and goodness of fit was attained between paramylon content and SSC-A for unstained cells. Lastly, the correlations and linear regression for KO525-A (labelled paramylon fluorescence) were strong and significant for both

strains. This indicates that there is positive relationship between the FCM fluorescence, SSC and FSC and paramylon and validated their use as measures of paramylon content in *E. gracilis*.

Fluorescence based detection of intracellular paramylon via FCM has not been previously established so there were no examples in the existing literature to make direct comparison as to the strength of the relationship between MFI and paramylon content. However, FCM analysis of microalgae has been undertaken in the context of oil production. These studies have predominately employed the fluorescence dye nile red and generally validated FCM analysis via correlation or linear regression against gravimetric or chromatographic determination of lipid/oil content. Depending on the microalga, type of oil/lipid and quantification method used, these studies have reported significant correlation coefficients (r values) between 0.79 and 0.97 and coefficients of determination (goodness of fit/ R^2 values) ranging from 0.6990 to 0.9336 [73, 163-165]. Using this as a benchmark/guide, the results of this work indicate that there was a fairly strong relationship between paramylon content and MFI (KO525), thus FCM could be effectively used to measure relative paramylon content in *E. gracilis*.

In addition to aniline blue fluorescence (KO525), side scatter (SSC) and forward scatter (FSC) were applied for analysis of paramylon content. SSC, which is considered to be indicative of intracellular complexity and granularity, had a stronger correlation with the paramylon content than KO525. Therefore, it is possible that in the interest of expediency, SSC alone could be used for paramylon content. Conversely, determination of paramylon could be enhanced through implementing multi-parametric analysis by combining both aniline blue fluorescence and SSC. For example, a multi-parametric FCM approach combining tagged lipid fluorescence (BODIPY[505/515]) and cellular opacity has been implemented by Guo, et al. [102] in the screening of *Euglena* strains for biofuel production. FSC of the unstained control cells for both strains studied here also had a fairly strong correlation with paramylon content. As mentioned previously, FSC signal is influenced by the size of the particle or cell passing through the excitation source (laser). The most likely explanation for the positive correlation is that as paramylon content in the cells increased or decreased, so did the overall size of the cells, which in turn affected the FSC signal intensity. However, the correlation of FSC from stained cells was lower than their unstained counterparts (i.e. the stained cells were smaller than unstained cells). This suggests that the staining/labelling process had a measurable impact on the scatter, and therefore the size and shape of the cells. Despite this, FSC could be applied as a third (indirect) parameter for the analysis of paramylon in *E. gracilis*.

4.4 **High-throughput analysis of paramylon in *E. gracilis* by flow cytometry**

Following correlation analysis, it was investigated whether FCM could be used to monitor paramylon content over a cultivation period of *E. gracilis* Z and *E. gracilis* var. *saccharophila,* and if FCM could identify variation in the paramylon content between cultivation times and strains. Results from paramylon per dry biomass (by PSA), KO525-A (by FCM) and SSC-A (by FCM) all indicated that there was a relatively high content of paramylon present on day 1 (17 h) and day 2 (41 h) of cultivation, followed by a steady decline over the course of the cultivation. However, from graphing the results, it was less clear if there was a difference in paramylon between the two strains.

A two-way ANOVA was then undertaken to establish whether there was a statistically significant difference in paramylon content and MFI between the cultivation times and *E. gracilis* strains. From the two-way ANOVA it was confirmed that there was a significant variation in paramylon content across cultivation times, such that cultivation time accounted for the largest percentage of total variation between samples. The two-way ANOVA also indicated that there was no significant difference in paramylon content between *E. gracilis* Z and *E. gracilis* var. *saccharophila* as measured by PSA. However, there was significant variation in MFI between the strains for labelled fluorescence (KO525) and SSC (control). It seems most likely that the large difference between strains in MFI which was only apparent for KO525 could be due to less efficient staining/fluorescent labelling of the var. *saccharophila* strain. Therefore, fluorescent labelling of various *E. gracilis* strains, including var. *saccharophila* will most likely require further optimisation. In regard to side scatter, the analysis found that there was a very small yet highly significant variation between the two strains (accounting for only 0.04113% of total variation in paramylon content). Thus, by measuring SSC, flow cytometry was able distinguish even small differences in paramylon content, where PSA method could not. This may be due to the MFI of SSC having a relatively small standard deviation between biological replicates since each run acquired thousands of data points. Comparatively, the standard deviation between biological replicates for the PSA assay was much larger. However, a limitation of the current FCM analysis was the time taken between each sample partially due to instrument availability. In this cultivation and analysis, paramylon content per dry biomass peaked at on day 1 (17 h). Thus, while the degradation/ utilisation of paramylon was assessed, the period of paramylon production was currently unable to be examined.

In summary, FCM measurement showed predominantly strong correlations with quantified paramylon, and from this work appear to be a valid relative measure of paramylon content in *E. gracilis*. A significant advantage of utilising FCM for the analysis of paramylon content is that it

allows assessment of microalgal production and growth to be streamlined. For instance, in assessing the production of paramylon and growth of *E. gracilis* on potato liquor medium Santek, et al. [36] undertook manual microscopic cell counts, FCM cell counts, gravimetric dry biomass quantification and gravimetric paramylon quantification. By utilising FCM for paramylon content as presented in this work, the process would be significantly streamlined since only a single analysis would be required. Thus, once optimised, the current FCM method is simpler (with or without fluorescent labelling), more time efficient and significantly higher-throughput than previous biochemical and gravimetric methods. These benefits are also greatly enhanced by the use of a fully automatic sampling instrument, enabling automated analysis of many thousands of cells per sample across a 96-well microplate, as opposed to the standard FCM process of loading a single tube at a time.

4.5   High-throughput analysis of chlorophyll in *E. gracilis* by flow cytometry

High-throughput FCM examination of chlorophyll fluorescence was conducted alongside analysis of paramylon content as an additional parameter in monitoring the metabolic state of the cells and to explore FCM as a tool for chlorophyll quantification. Correlations were examined to validate the MFI against quantification via chlorophyll precipitation and absorbance spectrophotometry. The results displayed strong positive correlations and goodness of fit between red light fluorescence emission (PC5.5 and PerCP) and chlorophyll content. This indicates that red light fluorescence corresponded to chlorophyll content and that FCM results could be confidently applied for assessment of chlorophyll in *E. gracilis Z* and var. *saccharophila*. Furthermore, while an appropriate internal standard such as chlorophyll beads were not available during this work, these could be implemented in future investigations for improved quantification of total chlorophyll content.

Following the comparison chlorophyll content and chlorophyll fluorescence, FCM and absorbance spectrophotometry were used to examine the chlorophyll content of the cells across their cultivation. When adjusted for cell concentration of cultures, chlorophyll content as assessed by spectrophotometry, FCM PerCP-A (Ex488 nm, Em690/50 nm) and FCM PC5.5 (Ex561 nm, Em690/50 nm) increased steadily over the cultivation period, with the *Z* strain having a higher content than var. *saccharophila* at each time point. Statistical analysis of these results via two-way ANOVA confirmed that both the cultivation time and strain had a significant effect on chlorophyll content and fluorescence. This revealed that as the cultures aged, the total chlorophyll content of the cultures increased, which suggests that FCM could be used as in indicator of relative pigment content, reliance of the cells on photosynthesis, and as a tool for improved process control.

4.5   Relationship between chlorophyll and paramylon in *E. gracilis*

Lastly, red fluorescence (PC5.5-A and PerCP-A) and side/right-angle scatter (SSC-A) were compared to examine whether FCM could be used to identify a relationship, if any between the chlorophyll and paramylon content. Results (Figure 16A) demonstrated that the median chlorophyll content per cell of both strains was initially relatively high at the beginning of the cultivation and dropped to its lowest point at day 3 (65 h). It seems most likely that this reflected a switch from a photoautotrophic state to a heterotrophic state as the cells were subcultured from the previous parent culture where the cell were relying on photosynthesis, to the fresh medium in the current cultivation, which contained glucose as a readily available carbon source. This was followed by a return to photoautotrophy, presumably once glucose in the medium had been depleted. However, this trend may also have been affected by population growth in the early cultivation period (see Figure 16B) as cells divided and had to develop new cellular components.

Chlorophyll and paramylon were compared once *E. gracilis Z* and var. *saccharophila* reached the stationary phase of their cultivation to avoid cell growth and division influencing the content in the cells. Correlation and linear regression analysis of chlorophyll MFI against cell side scatter (granularity) MFI indicated that there was a strong and highly significant negative relationship between chlorophyll and paramylon content. One possible explanation for this, is that the exposure to light during cultivation could have induced the utilisation of paramylon for cell growth and for the development of chlorophyll and photosynthetic apparatus as the cells switched from heterotrophy (feeding on glucose in the medium) to photoautotrophy. This hypothesis seems plausible considering previous research on paramylon degradation and utilization in *E. gracilis* [49, 63, 69, 70]. As in these previous studies, further investigation could be carried out by examining glucose content, the presence of paramylon synthesis and degradation enzymes and the behaviour of dark grown cells. The correlation and linear regression analysis conducted in this work, while highly significant, cannot imply a causative effect; therefore, it is unknown here whether the change in chlorophyll content was responsible for the reduction in the amount of paramylon or if the effect was the other way around. Nevertheless, the results presented in this work demonstrate that FCM can be successfully used for the high-throughput analysis of thousands of *E. gracilis* cells throughout their cultivation and can successfully employ multiple parameters at once to monitor paramylon and chlorophyll content and utilisation. This in turn can be used to infer the metabolic state of the cells. This approach has potential applications for screening highly productive stains, optimising cultivation conditions and for monitoring the metabolic state of cultures during production.

Chapter 5: Summary, conclusions and future directions

The microalgal protist *E. gracilis* holds promise as a nutritious source of food and dietary fibre, as well as a host for production of a range of valuable compounds including the β-1,3-glucan paramylon. Algal research has benefitted from the array of fluorescent dyes and detection instruments now available, which enable fluorescence based analysis of a wide range of cells, cellular compartments, molecules and biological processes. When implemented in conjunction with FCM and newly available automated sampling FCM instruments, fluorescence and light scatter based methods offer a powerful platform for the detection and analysis of many thousands of cells at a time.

Fluorescence and FCM based analysis methods have recently been implemented for the development of biotechnology processes in algae such as *E. gracilis* in the quest for sustainable production of biofuels [27, 102]. These methods are particularly valuable for working with *E. gracilis* due to a current scarcity of molecular and genetic tools available for the organism. Application of fluorescence and FCM methods for paramylon research and development has until now been noticeably absent. Part of this discrepancy, for example, could be attributed to the shortage of specific fluorescent dyes that target carbohydrates and glucans such as starch and paramylon. The overall goal of this investigation was to address this gap by developing methods for fluorescent labelling of paramylon and high-throughput analysis of *E. gracilis* via FCM. Specifically, this work aimed to improve current capabilities towards enhancing paramylon production. This was achieved by investigating alternative methods for rapid and efficient detection of compounds, monitoring of cultivation and the metabolic state of the cells and screening of strains.

The first area investigated was the fluorescent labelling of paramylon. The effectiveness of labelling was examined by fluorescence microscopy, and to the authors' knowledge, resulted in the first example of fluorescent labelling of intracellular paramylon in *Euglena*. This success was followed by investigation of the paramylon and chlorophyll content during mixotrophic (photo-heterotrophic) cultivation of *E. gracilis Z* and *E. gracilis* var. *saccharophila* strains by FCM. FCM results were validated against gravimetric and absorbance spectrophotometry quantification methods, and demonstrated successful detection and differentiation of paramylon and chlorophyll content between strains and across cultivation days. Lastly, while a conclusive statement cannot be made, the development of chlorophyll seems to be linked to the degradation of paramylon in *E. gracilis* and FCM analysis of chlorophyll fluorescence could be used to monitor metabolic state of cells throughout the cultivation. In light of these results it is evident that the fluorescence and FCM based

analysis presented here has potential as a high-throughput and efficient, multi-parametric method for the detection of paramylon content and monitoring of metabolic state in *E. gracilis*.

For the continued use and development of FCM for paramylon production in *E. gracilis* various avenues could be explored. For instance, in this investigation, side scatter analysis had a higher correlation with the paramylon content than the aniline blue fluorescence, thus, label free paramylon assessment could be a viable option. In addition, this would allow FCM analysis of paramylon in *E. gracilis* to be applied to bleached and dark/heterotrophically grown cells which were originally excluded due to higher levels of auto-fluorescence. Alternatively, fluorescent labelling of paramylon could be further optimised for improved multi-parametric analysis. This could include the use of β-glucan specific monoclonal antibodies which could be paired with a secondary fluorescent antibody that does not overlap with the cellular auto-fluorescence.

Besides use as a routine method for monitoring of paramylon production during cultivations, one future application for the FCM processes developed in this work is live sorting and development of overproducing strains. For example, FCM based cell sorting (fluorescence activated cells sorting: FACS) has recently been used for selective breeding of oil-rich *E. gracilis* for the production of biofuels [27]. In this case, *E. gracilis* cells were exposed to Fe-ion irradiation to create mutant strains, where upon the cells were repetitively cultivated, stained to induce fluorescence of intracellular lipids and isolated via FACS. By the end of the process a stable, lipid-rich mutant strain had been successfully developed, which contained on average 40% higher lipid content than the parent wild type strain. Similarly, the process developed here could be applied for screening large numbers of *Euglena* mutants or recombinants in order to identify the best over producers of paramylon. Finally, while this study has only focused on *Euglena gracilis*, the *Euglena* genus contain over 200 known species with common features [166], the majority of which have not yet been evaluated for biotechnological application. Recent research has shown, however, that some of these such as *Euglena anabaena* var. *minor* may also be strong candidates for paramylon production and other industrial applications [167]. As a result, fluorescence and FCM analysis of paramylon may not only allow examination and screening of *E. gracilis,* but also the abundant species and strains of *Euglena* that have yet to be explored.

References

[1] Andersen, R. A., *Algal culturing techniques*, Elsevier/Academic press, Boston, Mass. 2005.

[2] Cardozo, K. H. M., Guaratini, T., Barros, M. P., Falcão, V. R*., et al.*, Metabolites from algae with economical impact. *Comparative Biochemistry and Physiology Part C: Toxicology & Pharmacology* 2007, *146*, 60-78.

[3] Metting, B., Pyne, J. W., Biologically active compounds from microalgae. *Enzyme and Microbial Technology* 1986, *8*, 386-394.

[4] Borowitzka, M. A., Microalgae as sources of pharmaceuticals and other biologically active compounds. *Journal of Applied Phycology* 1995, *7*, 3-15.

[5] Pulz, O., Gross, W., Valuable products from biotechnology of microalgae. *Applied Microbiology and Biotechnology* 2004, *65*, 635-648.

[6] Becker, W., in: Richmond, A., Hu, Q. (Eds.), *Handbook of microalgal culture: biotechnology and applied phycology*, John Wiley & Sons 2013, pp. 461-503.

[7] Brown, M. R., Mular, M., Miller, I., Farmer, C., Trenerry, C., The vitamin content of microalgae used in aquaculture. *Journal of Applied Phycology* 1999, *11*, 247-255.

[8] Takeyama, H., Kanamaru, A., Yoshino, Y., Kakuta, H*., et al.*, Production of antioxidant vitamins, β-carotene, vitamin C, and vitamin E, by two-step culture of *Euglena gracilis* Z. *Biotechnology and Bioengineering* 1997, *53*, 185-190.

[9] Arad, S., Yaron, A., Natural pigments from red microalgae for use in foods and cosmetics. *Trends in Food Science & Technology* 1992, *3*, 92-97.

[10] Spolaore, P., Joannis-Cassan, C., Duran, E., Isambert, A., Commercial applications of microalgae. *Journal of Bioscience and Bioengineering* 2006, *101*, 87-96.

[11] Becker, E. W., Micro-algae as a source of protein. *Biotechnology Advances* 2007, *25*, 207-210.

[12] Chisti, Y., Biodiesel from microalgae. *Biotechnology Advances* 2007, *25*, 294-306.

[13] Krajčovič, J., Matej, V., Schwartzbach, S. D., Euglenoid flagellates: A multifaceted biotechnology platform. *Journal of Biotechnology* 2015, *202*, 135-145.

[14] Li, Y., Horsman, M., Wu, N., Lan, C. Q., Dubois-Calero, N., Biofuels from microalgae. *Biotechnology Progress* 2008, *24*, 815-820.

[15] Raja, R., Hemaiswarya, S., Kumar, N. A., Sridhar, S., Rengasamy, R., A perspective on the biotechnological potential of microalgae. *Critical Reviews in Microbiology* 2008, *34*, 77-88.

[16] Borowitzka, M. A., Commercial production of microalgae: ponds, tanks, tubes and fermenters. *Journal of Biotechnology* 1999, *70*, 313-321.

[17] Shimogawara, K., Fujiwara, S., Grossman, A., Usuda, H., High-efficiency transformation of *Chlamydomonas reinhardtii* by electroporation. *Genetics* 1998, *148*, 1821-1828.

[18] Coll, J. M., Methodologies for transferring DNA into eukaryotic microalgae: a review. *2006* 2006, *4*, 316-330.

[19] Rosenberg, J. N., Oyler, G. A., Wilkinson, L., Betenbaugh, M. J., A green light for engineered algae: redirecting metabolism to fuel a biotechnology revolution. *Current Opinion in Biotechnology* 2008, *19*, 430-436.

[20] Courchesne, N. M. D., Parisien, A., Wang, B., Lan, C. Q., Enhancement of lipid production using biochemical, genetic and transcription factor engineering approaches. *Journal of Biotechnology* 2009, *141*, 31-41.

[21] Khozin-Goldberg, I., Cohen, Z., Unraveling algal lipid metabolism: Recent advances in gene identification. *Biochimie* 2011, *93*, 91-100.

[22] Blatti, J. L., Beld, J., Behnke, C. A., Mendez, M*., et al.*, Manipulating fatty acid biosynthesis in microalgae for biofuel through protein-protein interactions. *PLOS ONE* 2012, *7*, e42949.

[23] Chisti, Y., Constraints to commercialization of algal fuels. *Journal of Biotechnology* 2013, *167*, 201-214.

[24] Dunahay, T. G., Jarvis, E. E., Dais, S. S., Roessler, P. G., in: Wyman, C. E., Davison, B. H. (Eds.), *Seventeenth symposium on biotechnology for fuels and chemicals: presented as volumes 57 and 58 of Applied Biochemistry and Biotechnology*, Humana Press, Totowa, NJ 1996, pp. 223-231.

[25] Kindle, K. L., High-frequency nuclear transformation of *Chlamydomonas reinhardtii*. *Proceedings of the National Academy of Sciences* 1990, *87*, 1228-1232.

[26] Schiedlmeier, B., Schmitt, R., Müller, W., Kirk, M. M*., et al.*, Nuclear transformation of *Volvox carteri*. *Proceedings of the National Academy of Sciences* 1994, *91*, 5080-5084.

[27] Yamada, K., Suzuki, H., Takeuchi, T., Kazama, Y*., et al.*, Efficient selective breeding of live oil-rich *Euglena gracilis* with fluorescence-activated cell sorting. *Scientific Reports* 2016, *6*, 26327.

[28] Barsanti, L., Vismara, R., Passarelli, V., Gualtieri, P., Paramylon (β-1,3-glucan) content in wild type and WZSL mutant of *Euglena gracilis*. Effects of growth conditions. *Journal of Applied Phycology* 2001, *13*, 59-65.

[29] Ogawa, T., Tamoi, M., Kimura, A., Mine, A*., et al.*, Enhancement of photosynthetic capacity in *Euglena gracilis* by expression of cyanobacterial fructose-1,6-/sedoheptulose-1,7-bisphosphatase leads to increases in biomass and wax ester production. *Biotechnology for Biofuels* 2015, *8*, 80.

[30] Wolken, J. J., *Euglena: an experimental organism for biochemical and biophysical studies*, New York : Appleton-Century Crofts, New York 1967.

[31] Šantek, B. i., Felski, M., Friehs, K., Lotz, M., Flaschel, E., Production of paramylon, a β-1,3-glucan, by heterotrophic cultivation of *Euglena gracilis* on a synthetic medium. *Engineering in Life Sciences* 2009, *9*, 23-28.

[32] Ahmadinejad, N., Dagan, T., Martin, W., Genome history in the symbiotic hybrid *Euglena gracilis*. *Gene* 2007, *402*, 35-39.

[33] Hofmann, C., Bouck, B., Immunological and structural evidence for patterned intussusceptive surface growth in a unicellular organism. A postulated role for submembranous proteins and microtubules. *The Journal of Cell Biology* 1976, *69*, 693-715.

[34] Sommer, J. R., The ultrastructure of the pellicle complex of *Euglena gracilis*. *The Journal of Cell Biology* 1965, *24*, 253-257.

[35] Lefort-Tran, M., Pouphile, M., Freyssinet, G., Pineau, B., Structural and functional significance of the chloroplast envelope of *Euglena*: immunocytological and freeze fracture study. *Journal of Ultrastructure Research* 1980, *73*, 44-63.

[36] Santek, B., Friehs, K., Lotz, M., Flaschel, E., Production of paramylon, a β-1,3-glucan, by heterotrophic growth of *Euglena gracilis* on potato liquor in fed-batch and repeated-batch mode of cultivation. *Engineering in Life Sciences* 2012, *12*, 89-94.

[37] Schantz, R., Schantz, M.-L., Duranton, H., Changes in amino acid and peptide composition of *Euglena gracilis* cells during chloroplast development. *Plant Science Letters* 1975, *5*, 313-324.

[38] Meyer, A., Cirpus, P., Ott, C., Schlecker, R*., et al.*, Biosynthesis of docosahexaenoic acid in *Euglena gracilis*: Biochemical and molecular evidence for the involvement of a Δ4-fatty acyl group desaturase. *Biochemistry* 2003, *42*, 9779-9788.

[39] Bouck, G. B., Rosiere, T. K., Levasseur, P. J., in: Bloodgood, R. A. (Ed.), *Ciliary and Flagellar Membranes*, Springer US, Boston, MA 1990, pp. 65-90.

[40] Einicker-Lamas, M., Antunes Mezian, G., Benevides Fernandes, T., Silva, F. L. S*., et al.*, *Euglena gracilis* as a model for the study of Cu2+ and Zn2+ toxicity and accumulation in eukaryotic cells. *Environmental Pollution* 2002, *120*, 779-786.

[41] Häder, D.-P., Rosum, A., Schäfer, J., Hemmersbach, R., Graviperception in the flagellate *Euglena gracilis* during a shuttle space flight. *Journal of Biotechnology* 1996, *47*, 261-269.

[42] Nakano, Y., Miyataka, K., Yamaji, R., Nishizawa, A*., et al.*, A protist, *Euglena gracilis Z*, functions as a sole nutrient source in a closed ecosystem. *Eco-Engineering* 1995, *8*, 7-12.

[43] Kusmic, C., Barsacchi, R., Barsanti, L., Gualtieri, P., Passarelli, V., *Euglena gracilis* as source of the antioxidant vitamin E. Effects of culture conditions in the wild strain and in the natural mutant WZSL. *Journal of Applied Phycology* 1998, *10*, 555-559.

[44] Chae, S. R., Hwang, E. J., Shin, H. S., Single cell protein production of *Euglena gracilis* and carbon dioxide fixation in an innovative photo-bioreactor. *Bioresource Technology* 2006, *97*, 322-329.

[45] Kitaya, Y., Azuma, H., Kiyota, M., Effects of temperature, CO_2/O_2 concentrations and light intensity on cellular multiplication of microalgae, *Euglena gracilis*. *Advances in Space Research* 2005, *35*, 1584-1588.

[46] Lynch, V. H., Calvin, M., CO_2 fixation by *Euglena*. *Annals of the New York Academy of Sciences* 1953, *56*, 890-900.

[47] Kitaya, Y., Kibe, S., Oguchi, M., Tanaka, H.*, et al.*, Effects of CO_2 and O_2 concentrations and light intensity on growth of microalgae (*Euglena gracilis*) in CELSS. *Life support & biosphere science : international journal of earth space* 1998, *5*, 243-247.

[48] Briand, J., Calvayrac, R., Paramylon synthesis in heterotrophic and photoheterotrophic *Euglena* (euglenophyceae). *Journal of Phycology* 1980, *16*, 234-239.

[49] Sumida, S., Ehara, T., Osafune, T., Hase, E., Ammonia- and light-induced degradation of paramylum in *Euglena gracilis*. *Plant and Cell Physiology* 1987, *28*, 1587-1592.

[50] Clarke, A. E., Stone, B. A., Structure of the paramylon from *Euglena gracilis*. *Biochimica et Biophysica Acta* 1960, *44*, 161-163.

[51] Monfils, A. K., Triemer, R. E., Bellairs, E. F., Characterization of paramylon morphological diversity in photosynthetic euglenoids (Euglenales, Euglenophyta). *Phycologia* 2011, *50*, 156-169.

[52] Watanabe, T., Shimada, R., Matsuyama, A., Yuasa, M.*, et al.*, Antitumor activity of the β-glucan paramylon from *Euglena* against preneoplastic colonic aberrant crypt foci in mice. *Food & Function* 2013, *4*, 1685-1690.

[53] Sugiyama, A., Hata, S., Suzuki, K., Yoshida, E.*, et al.*, Oral administration of paramylon, a β-1,3-d-glucan isolated from *Euglena gracilis Z* inhibits development of atopic dermatitis-like skin lesions in nc/nga mice. *Journal of Veterinary Medical Science* 2010, *72*, 755-763.

[54] Koizumi, N., Sakagami, H., Utsumi, A., Fujinaga, S.*, et al.*, Anti-HIV (human immunodeficiency virus) activity of sulfated paramylon. *Antiviral Research* 1993, *21*, 1-14.

[55] Sugiyama, A., Suzuki, K., Mitra, S., Arashida, R.*, et al.*, Hepatoprotective effects of paramylon, a β-1, 3-d-glucan isolated from *Euglena gracilis Z*, on acute liver injury induced by carbon tetrachloride in rats. *Journal of Veterinary Medical Science* 2009, *71*, 885-890.

[56] Wang, L., Behr, S. R., Newman, R. K., Newman, C. W., Comparative cholesterol-lowering effects of barley β-glucan and barley oil in golden syrian hamsters. *Nutrition Research* 1997, *17*, 77-88.

[57] Wood, P. J., Evaluation of oat bran as a soluble fibre source. Characterization of oat β-glucan and its effects on glycaemic response. *Carbohydrate Polymers* 1994, *25*, 331-336.

[58] Chan, G. C.-F., Chan, W. K., Sze, D. M.-Y., The effects of β-glucan on human immune and cancer cells. *Journal of Hematology & Oncology* 2009, *2*, 25.

[59] Rodríguez-Zavala, J. S., Ortiz-Cruz, M. A., Mendoza-Hernández, G., Moreno-Sánchez, R., Increased synthesis of α-tocopherol, paramylon and tyrosine by *Euglena gracilis* under conditions of high biomass production. *Journal of Applied Microbiology* 2010, *109*, 2160-2172.

[60] Cook, J. R., Adaptations in growth and division in *Euglena* effected by energy supply. *Journal of Eukaryotic Microbiology* 1963, *10*, 436-444.

[61] Ivušić, F., Šantek, B., Optimization of complex medium composition for heterotrophic cultivation of *Euglena gracilis* and paramylon production. *Bioprocess and Biosystems Engineering* 2015, *38*, 1103-1112.

[62] Kawabata, A., Miyatake, K., Kitaoka, S., Effect of temperature on the contents of the two energy-reserve substances, paramylon and wax esters, in *Euglena gracilis*. *The Journal of Protozoology* 1982, *29*, 421-423.

[63] Kiss, J. Z., Vasoconcelos, A. C., Triemer, R. E., Paramylon synthesis and chloroplast structure associateed with nutrient levels in *Euglena* (euglenophyceae)1. *Journal of Phycology* 1986, *22*, 327-333.

[64] Vogel, K., Barber, A. A., Degradation of paramylon by *Euglena gracilis*. *Journal of Eukaryotic Microbiology* 1968, *15*, 657-662.

[65] Coleman, L. W., Rosen, B. H., Schwartzbach, S. D., Environmental control of carbohydrate and lipid synthesis in *Euglena*. *Plant and Cell Physiology* 1988, *29*, 423-432.

[66] Inui, H., Miyatake, K., Nakano, Y., Kitaoka, S., Wax ester fermentation in *Euglena gracilis*. *FEBS Letters* 1982, *150*, 89-93.

[67] Schneider, T., Betz, A., Waxmonoester fermentation in *Euglena gracilis* T. Factors favouring the synthesis of odd-numbered fatty acids and alcohols. *Planta* 1985, *166*, 67-73.

[68] Nishimura, M., Huzisige, H., Studies on the chlorophyll formation in *Euglena gracilis* with special reference to the action spectrum if the process. *The Journal of Biochemistry* 1959, *46*, 225-234.

[69] Dwyer, M. R., Smillie, R. M., A light-induced β-1,3-glucan breakdown associated with the differentiation of chloroplasts in *Euglena gracilis*. *Biochimica et Biophysica Acta (BBA) - Bioenergetics* 1970, *216*, 392-401.

[70] Dwyer, M. R., Smydzuk, J., Smillie, R. M., Synthesis and breakdown bf β-1,3-glucan In *Euglena Gracilis* during growth and carbon depletion. *Australian Journal of Biological Sciences* 1970, *23*, 1005-1014.

[71] Hallick, R. B., Hong, L., Drager, R. G., Favreau, M. R*., et al.*, Complete sequence of *Euglena gracilis* chloroplast DNA. *Nucleic Acids Research* 1993, *21*, 3537-3544.

[72] Doan, T. T. Y. E. N., Obbard, J. P., Enhanced lipid production in *Nannochloropsis sp.* using fluorescence-activated cell sorting. *GCB Bioenergy* 2011, *3*, 264-270.

[73] Cagnon, C., Mirabella, B., Nguyen, H. M., Beyly-Adriano, A*., et al.*, Development of a forward genetic screen to isolate oil mutants in the green microalga *Chlamydomonas reinhardtii*. *Biotechnology for Biofuels* 2013, *6*, 178.

[74] Cook, J. R., Quantitative measurement of paramylum in *Euglena gracilis*. *Journal of Eukaryotic Microbiology* 1967, *14*, 634-636.

[75] Johnson, I., *The molecular probes handbook: A guide to fluorescent probes and labeling technologies, 11th edition*, Life Technologies Corporation 2010.

[76] Johnson, I., Review: Fluorescent probes for living cells. *The Histochemical Journal* 1998, *30*, 123-140.

[77] Ghetti, F., Colombetti, G., Lenci, F., Campani, E*., et al.*, Fluorescence of *Euglena gracilis* photoreceptor pigment: an in vivo microspectrofluorometric study. *Photochemistry and Photobiology* 1985, *42*, 29-33.

[78] Lichtman, J. W., Conchello, J.-A., Fluorescence microscopy. *Nature Methods* 2005, *2*, 910-919.

[79] Shapiro, H. M., *Practical flow cytometry*, John Wiley & Sons, Hoboken, New Jersey 2005.

[80] Widholm, J. M., The use of fluorescein diacetate and phenosafranine for determining viability of cultured plant cells. *Stain Technology* 1972, *47*, 189-194.

[81] Tsien, R. Y., The green fluorescent protein. *Annu. Rev. Biochem.* 1998, *67*, 509-544.

[82] Tsien, R. Y., New calcium indicators and buffers with high selectivity against magnesium and protons: design, synthesis, and properties of prototype structures. *Biochemistry* 1980, *19*, 2396-2404.

[83] Grynkiewicz, G., Poenie, M., Tsien, R. Y., A new generation of Ca2+ indicators with greatly improved fluorescence properties. *Journal of Biological Chemistry* 1985, *260*, 3440-3450.

[84] Honig, M. G., Hume, R. I., DiI and DiO: versatile fluorescent dyes for neuronal labelling and pathway tracing. *Trends in Neurosciences* 1989, *12*, 333-341.

[85] Gross, D., Loew, L. M., Chapter 7 Fluorescent indicators of membrane potential: microspectrofluorometry and imaging. *Methods in Cell Biology* 1989, *30*, 193-218.

[86] Nicklisch, A., Steinberg, C. E. W., RNA/protein and RNA/DNA ratios determined by flow cytometry and their relationship to growth limitation of selected planktonic algae in culture. *European Journal of Phycology* 2009, *44*, 297-308.

[87] Robinson, J. P., Carter, W. O., Narayanan, P. K., Chapter 28 Oxidative product formation analysis by flow cytometry. *Methods in Cell Biology* 1994, *41*, 437-447.

[88] Koley, D., Bard, A. J., Triton X-100 concentration effects on membrane permeability of a single HeLa cell by scanning electrochemical microscopy (SECM). *Proceedings of the National Academy of Sciences of the United States of America* 2010, *107*, 16783-16787.

[89] Hyka, P., Lickova, S., Přibyl, P., Melzoch, K., Kovar, K., Flow cytometry for the development of biotechnological processes with microalgae. *Biotechnology Advances* 2013, *31*, 2-16.

[90] Yentsch, C. S., Yentsch, C. M., Single cell analysis in biological oceanography and its evolutionary implications. *Journal of Plankton Research* 2008, *30*, 107-117.

[91] Sosik, H. M., Olson, R. J., Automated taxonomic classification of phytoplankton sampled with imaging-in-flow cytometry. *Limnology and Oceanography: Methods* 2007, *5*, e216.

[92] Collier, J., Campbell, L., *Molecular Ecology of Aquatic Communities*, Springer 1999, pp. 33-53.

[93] Davey, H. M., *Advanced flow cytometry: Applications in biological research*, Springer 2003, pp. 91-97.

[94] Davey, H. M., Kell, D. B., Flow cytometry and cell sorting of heterogeneous microbial populations: the importance of single-cell analyses. *Microbiological Reviews* 1996, *60*, 641-696.

[95] An, G.-H., Bielich, J., Auerbach, R., Johnson, E. A., Isolation and characterization of carotenoid hyperproducing mutants of yeast by flow cytometry and cell sorting. *Nature Biotechnology* 1991, *9*, 70-73.

[96] Barque, J. P., Abahamid, A., Bourezgui, Y., Chacun, H., Bonaly, J., Growth responses of achlorophyllous *Euglena gracilis* to selected concentrations of cadmium and pentachlorophenol. *Archives of Environmental Contamination and Toxicology* 1995, *28*, 8-12.

[97] Bonaly, J., Mestre, J. C., Flow fluorometric study of DNA content in nonproliferative *Euglena gracilis* cells and during proliferation. *Cytometry* 1981, *2*, 35-38.

[98] Lefort-Tran, M., Bre, M. H., Pouphile, M., Manigault, P., DNA flow cytometry of control *Euglena* and cell cycle blockade of vitamin B12-starved cells. *Cytometry* 1987, *8*, 46-54.

[99] Bonaly, J., Brochiero, E., Cell-surface changes in cadmium-resistant *Euglena*: studies using lectin-binding techniques and flow cytometry. *Bulletin of Environmental Contamination and Toxicology* 1994, *52*, 54-60.

[100] Bre, M. H., Leforttran, M., Obrenovitch, A., Monsigny, M., Detection of *Euglena* cell-surface carbohydrates by lectins - alterations related to vitamin-b12 deficiency. *European Journal of Cell Biology* 1984, *35*, 273-278.

[101] Mares, D., Bonora, A., Sacchetti, G., Rubini, M., Romagnoli, C., Protoanemonin-induced cytotoxic effects in *Euglena gracilis*. *Cell Biology International* 1997, *21*, 397-404.

[102] Guo, B., Lei, C., Ito, T., Jiang, Y., *et al.*, High-throughput accurate single-cell screening of *Euglena gracilis* with fluorescence-assisted optofluidic time-stretch microscopy. *PLOS ONE* 2016, *11*, e0166214.

[103] Lei, C., Ito, T., Ugawa, M., Nozawa, T., *et al.*, High-throughput label-free image cytometry and image-based classification of live *Euglena gracilis*. *Biomedical optics express* 2016, *7*, 2703-2708.

[104] Trask, B. J., Engh, G. J. v. d., Elgershuizen, J. H. B. W., Analysis of phytoplankton by flow cytometry. *Cytometry* 1982, *2*, 258-264.

[105] Cunningham, A., Buonnacorsi, G. A., Narrow-angle forward light-scattering from individual algal cells - implications for size and shape-discrimination in flow-cytometry. *Journal of Plankton Research* 1992, *14*, 223-234.

[106] Koch, A. L., Robertson, B. R., Button, D. K., Deduction of the cell volume and mass from forward scatter intensity of bacteria analyzed by flow cytometry. *Journal of Microbiological Methods* 1996, *27*, 49-61.

[107] Demers, S., Roy, S., Gagnon, R., Vignault, C., Rapid light-induced changes in cell fluorescence and in xanthophyll-cycle pigments of *Alexandrium excavatum* (Dinophyceae) and *Thalassiosira pseudonana* (Bacillariophyceae): a photo-protection mechanism. *Marine Ecology Progress Series* 1991, 185-193.

[108] Leya, T., Rahn, A., Lütz, C., Remias, D., Response of arctic snow and permafrost algae to high light and nitrogen stress by changes in pigment composition and applied aspects for biotechnology. *FEMS Microbiology Ecology* 2009, *67*, 432-443.

[109] Liu, B.-H., Lee, Y.-K., Secondary carotenoids formation by the green alga *Chlorococcum sp.* *Journal of Applied Phycology* 2000, *12*, 301-307.

[110] Collier, J. L., Flow cytometry and the single cell in phycology. *Journal of Phycology* 2000, *36*, 628-644.

[111] Phinney, D. A., Cucci, T. L., Flow cytometry and phytoplankton. *Cytometry* 1989, *10*, 511-521.

[112] Zhang, M., Kong, F., Shi, X., Xing, P., Tan, X., Differences in responses to darkness between *Microcystis aeruginosa* and *Chlorella pyrenoidosa*. *Journal of Freshwater Ecology* 2007, *22*, 93-99.

[113] Reckermann, M., Flow sorting in aquatic ecology. *Scientia Marina* 2000, *64*, 235-246.

[114] Xiong, W., Liu, L., Wu, C., Yang, C., Wu, Q., 13C-tracer and gas chromatography-mass spectrometry analyses reveal metabolic flux distribution in the oleaginous microalga *Chlorella protothecoides*. *Plant physiology* 2010, *154*, 1001-1011.

[115] Gouveia, L., Marques, A. E., da Silva, T. L., Reis, A., *Neochloris oleabundans* UTEX #1185: a suitable renewable lipid source for biofuel production. *Journal of Industrial Microbiology & Biotechnology* 2009, *36*, 821-826.

[116] Yang, Y.-P., Juang, Y.-S., Hsu, B.-D., A quick method for assessing chloroplastic starch granules by flow cytometry. *Journal of Plant Physiology* 2002, *159*, 103-106.

[117] Kwok, A. C. M., Wong, J. T. Y., Cellulose synthesis is coupled to cell cycle progression at G1 in the dinoflagellate *Crypthecodinium cohnii*. *Plant Physiology* 2003, *131*, 1681-1691.

[118] Kwok, A. C. M., Wong, J. T. Y., The activity of a wall-bound cellulase is required for and is coupled to cell cycle progression in the dinoflagellate *Crypthecodinium cohnii*. *The Plant Cell* 2010, *22*, 1281-1298.

[119] Davey, H. M., Life, death, and in-between: meanings and methods in microbiology. *Applied Environmental Microbiology* 2011, *77*, 5571-5576.

[120] Veldhuis, M., Kraay, G., Timmermans, K., Cell death in phytoplankton: correlation between changes in membrane permeability, photosynthetic activity, pigmentation and growth. *European Journal of Phycology* 2001, *36*, 167-177.

[121] Jochem, F. J., Dark survival strategies in marine phytoplankton assessed by cytometric measurement of metabolic activity with fluorescein diacetate. *Marine Biology* 1999, *135*, 721-728.

[122] Sensen, C. W., Heimann, K., Melkonian, M., The production of clonal and axenic cultures of microalgae using fluorescence-activated cell sorting. *European Journal of Phycology* 1993, *28*, 93-97.

[123] Surek, B., Melkonian, M., CCAC - Culture collection of algae at the university of cologne: a new collection of axenic algae with emphasis on flagellates. *Nova Hedwigia* 2004, *79*, 77-92.

[124] Sinigalliano, C. D., Winshell, J., Guerrero, M. A., Scorzetti, G.*, et al.*, Viable cell sorting of dinoflagellates by multiparametric flow cytometry. *Phycologia* 2009, *48*, 249-257.

[125] Mendoza, H., De la Jara, A., Freijanes, K., Carmona, L.*, et al.*, Characterization of *Dunaliella salina* strains by flow cytometry: a new approach to select carotenoid hyperproducing strains. *Electronic Journal of Biotechnology* 2008, *11*, 5-6.

[126] Yamada, K., Kazama, Y., Mitra, S., Marukawa, Y.*, et al.*, Production of a thermal stress resistant mutant *Euglena gracilis* strain using Fe-ion beam irradiation. *Bioscience, Biotechnology, and Biochemistry* 2016, *80*, 1650-1656.

[127] Smith, M. M., McCully, M. E., A critical evaluation of the specificity of aniline blue induced fluorescence. *Protoplasma* 1978, *95*, 229-254.

[128] Evans, N. A., Hoyne, P. A., Stone, B. A., Characteristics and specificity of the interaction of a fluorochrome from aniline blue (sirofluor) with polysaccharides. *Carbohydrate Polymers* 1984, *4*, 215-230.

[129] Bougourd, S., Marrison, J., Haseloff, J., An aniline blue staining procedure for confocal microscopy and 3D imaging of normal and perturbed cellular phenotypes in mature *Arabidopsis* embryos. *The Plant Journal* 2000, *24*, 543-550.

[130] Brundrett, M. C., Enstone, D. E., Peterson, C. A., A berberine-aniline blue fluorescent staining procedure for suberin, lignin, and callose in plant tissue. *Protoplasma* 1988, *146*, 133-142.

[131] Ko, Y.-T., Lin, Y.-L., 1,3-β-Glucan quantification by a fluorescence microassay and analysis of its distribution in foods. *Journal of Agricultural and Food Chemistry* 2004, *52*, 3313-3318.

[132] Wood, P. J., Specificity in the interaction of direct dyes with polysaccharides. *Carbohydrate Research* 1980, *85*, 271-287.

[133] Maeda, H., Ishida, N., Specificity of binding of hexopyranosyl polysaccharides with fluorescent brightener. *The Journal of Biochemistry* 1967, *62*, 276-278.

[134] Hughes, J., McCully, M. E., The use of an optical brightener in the study of plant structure. *Stain Technology* 1975, *50*, 319-329.

[135] Fischer, J. M. C., Peterson, C. A., Bols, N. C., A new fluorescent test for cell vitality using calcofluor white M2R. *Stain Technology* 1985, *60*, 69-79.

[136] Nakano, Y., Urade, Y., Urade, R., Kitaoka, S., Isolation, purification, and characterization of the pellicle of *Euglena gracilis* Z. *The Journal of Biochemistry* 1987, *102*, 1053-1063.

[137] Jeffrey, S. W., Humphrey, G. F., New spectrophotometric equations for determining chlorophylls a, b, c1 and c2 in higher plants, algae and natural phytoplankton. *Biochemie und Physiologie der Pflanzen* 1975, *167*, 191-194.

[138] Holm-Hansen, O., Lorenzen, C. J., Holmes, R. W., Strickland, J. D. H., Fluorometric determination of chlorophyll. *ICES Journal of Marine Science* 1965, *30*, 3-15.

[139] Hagiwara, S.-y., Takahashi, M., Yamagishi, A., Zhang, Y., Goto, K., Novel findings regarding photoinduced commitments of G1-, S- and G2-phase cells to cell-cycle transitions in darkness and dark-induced G1-, S- and G2-phase arrests in *Euglena*. *Photochemistry and Photobiology* 2001, *74*, 726-733.

[140] Hutner, S. H., Bach, M. K., Ross, G. T. M., A sugar-containing basal medium for vitamin b12-assay with *Euglena*; application to body fluids*. *The Journal of Protozoology* 1956, *3*, 101-112.

[141] DuBois, M., Gilles, K. A., Hamilton, J. K., Rebers, P. A., Smith, F., Colorimetric method for determination of sugars and related substances. *Analytical Chemistry* 1956, *28*, 350-356.

[142] Herburger, K., Holzinger, A., Aniline blue and calcofluor white staining of callose and cellulose in the streptophyte green algae *Zygnema* and *Klebsormidium*. *Bio-protocol* 2016, *6*, e1969.

[143] Uniacke, J., Colón-Ramos, D., Zerges, W., in: Gerst, J. E. (Ed.), *RNA Detection and Visualization: Methods and Protocols*, Humana Press, Totowa, NJ 2011, pp. 15-29.

[144] Jamur, M. C., Oliver, C., in: Oliver, C., Jamur, M. C. (Eds.), *Immunocytochemical Methods and Protocols*, Humana Press, Totowa, NJ 2010, pp. 63-66.

[145] Smith, M. M., McCully, M. E., Enhancing aniline blue fluorescent staining of cell wall structures. *Stain Technology* 1978, *53*, 79-85.

[146] Ogawa, K., Dohmaru, T., Yui, T., Dependence of complex formation of (1→ 3)-β-D-glucan with congo red on temperature in alkaline solutions. *Bioscience, Biotechnology, and Biochemistry* 1994, *58*, 1870-1872.

[147] Rasconi, S., Jobard, M., Jouve, L., Sime-Ngando, T., Use of calcofluor white for detection, identification, and quantification of phytoplanktonic fungal parasites. *Applied and Environmental Microbiology* 2009, *75*, 2545-2553.

[148] Schneider, C. A., Rasband, W. S., Eliceiri, K. W., NIH Image to ImageJ: 25 years of image analysis. *Nature Methods* 2012, *9*, 671-675.

[149] Schindelin, J., Arganda-Carreras, I., Frise, E., Kaynig, V.*, et al.*, Fiji: an open-source platform for biological-image analysis. *Nature Methods* 2012, *9*, 676-682.

[150] Barsanti, L., Passarelli, V., Walne, P. L., Gualtieri, P., The photoreceptor protein of *Euglena gracilis*. *FEBS Letters* 2000, *482*, 247-251.

[151] Schmidt, W., Galland, P., Senger, H., Furuya, M., Microspectrophotometry of *Euglena gracilis*. *Planta* 1990, *182*, 375-381.

[152] Brodhun, B., Hader, D.-P., Photoreceptor proteins and pigments in the paraflagellar body of the flagellate *Euglena gracilis*. *Photochemistry and Photobiology* 1990, *52*, 865-871.

[153] Brody, M., Brody, S. S., Levine, J. H., Fluorescence changes during chlorophyll formation in *Euglena gracilis* (and other organisms) and an estimate of lamellar area as a function of age. *Journal of Eukaryotic Microbiology* 1965, *12*, 465-476.

[154] Doege, M., Ohmann, E., Tschiersch, H., Chlorophyll fluorescence quenching in the alga *Euglena gracilis*. *Photosynthesis Research* 2000, *63*, 159-170.

[155] Cason, J. E., A rapid one-step Mallory-Heidenhain stain for connective tissue. *Stain Technology* 1950, *25*, 225-226.

[156] Kirk, J. T. O., Juniper, B. E., The fine structure of the pellicle of *Euglena gracilis*. *Journal of the Royal Microscopical Society* 1964, *82*, 205-210.

[157] Stone, B. A., Evans, N. A., Bonig, I., Clarke, A. E., The application of Sirofluor, a chemically defined fluorochrome from aniline blue for the histochemical detection of callose. *Protoplasma* 1984, *122*, 191-195.

[158] Meikle, P. J., Hoogenraad, N. J., Bonig, I., Clarke, A. E., Stone, B. A., A (1→3,1→4)-β-glucan-specific monoclonal antibody and its use in the quantitation and immunocytochemical location of (1→3,1→4)-β-glucans. *The Plant Journal* 1994, *5*, 1-9.

[159] Kiss, J. Z., Vasconcelos, A. C., Triemer, R. E., Structure of the euglenoid storage carbohydrate, paramylon. *American Journal of Botany* 1987, *74*, 877-882.

[160] Kiss, J. Z., Roberts, E. M., Brown, R. M., Triemer, R. E., X-ray and dissolution studies of paramylon storage granules from *Euglena*. *Protoplasma* 1988, *146*, 150-156.

[161] Kiss, J. Z., Vasconcelos, A. C., Triemer, R. E., The intramembranous particle profile of the paramylon membrane during paramylon synthesis in *Euglena* (euglenophyceae). *Journal of Phycology* 1988, *24*, 152-157.

[162] Young, S.-H., Dong, W.-J., Jacobs, R. R., Observation of a partially opened triple-helix conformation in 1→3-β-glucan by fluorescence resonance energy transfer spectroscopy. *Journal of Biological Chemistry* 2000, *275*, 11874-11879.

[163] de la Jara, A., Mendoza, H., Martel, A., Molina, C.*, et al.*, Flow cytometric determination of lipid content in a marine dinoflagellate, *Crypthecodinium cohnii. Journal of Applied Phycology* 2003, *15*, 433-438.

[164] da Silva, T. L., Reis, A., Medeiros, R., Oliveira, A. C., Gouveia, L., Oil production towards biofuel from autotrophic microalgae semicontinuous cultivations monitorized by flow cytometry. *Applied Biochemistry and Biotechnology* 2009, *159*, 568-578.

[165] Cooksey, K. E., Guckert, J. B., Williams, S. A., Callis, P. R., Fluorometric determination of the neutral lipid content of microalgal cells using nile red. *Journal of Microbiological Methods* 1987, *6*, 333-345.

[166] Johnson, L. P., in: Buetow, D. E. (Ed.), *The Biology of Euglena Volume 1: general biology and ultrastructure*, New York : Academic Press, New York 1968, pp. 1-27.

[167] Suzuki, K., Mitra, S., Iwata, O., Ishikawa, T.*, et al.*, Selection and characterization of *Euglena anabaena* var. *minor* as a new candidate *Euglena* species for industrial application. *Bioscience, Biotechnology, and Biochemistry* 2015, *79*, 1730-1736.